



# Quantum processes with indefinite causal order on time-delocalized subsystems

Shift basis distinguishability using time-delocalized realization of the Lugano process

Mémoire présenté en vue de l'obtention du diplôme  
d'Ingénieur Civil Physicien à finalité spécialisée

**Eliot Niedercorn**

Supervisor

Prof. Ognian Oreshkov

Co-supervisors

Dr. Julian Wechs and Dr. Ravi Kunjwal

Research Group

Centre for Quantum Information and Communication (QuIC)

Academic Year

2022 - 2023

# *Abstract*

École polytechnique de Bruxelles

Centre for Quantum Information and Communication (QuIC)

Master en Ingénieur Civil Physicien

## **Shift basis distinguishability using time-delocalized realization of the Lugano process**

by Eliot Niedercorn

The process matrix formalism offers a description of quantum theory without a well-defined causal structure, which could potentially have relevance for quantum gravity. This formalism allows for the description of causally indefinite processes, with one notable example being the quantum switch, which has been experimentally realized and has demonstrated computational advantages that are unreachable in situations with a definite causal structure.

This thesis focuses on another causally indefinite process, known as the Lugano process, which has been proven to achieve something impossible by quantum nonlocality without entanglement (QNWE) in a situation with a well-defined causal order: the establishment of a protocol using only local operations and classical communication (LOCC) that implements a complete measurement of a set of unentangled orthogonal states called the Shift basis.

The main objective of this master's thesis is to investigate the implementation of this protocol in a temporally ordered circuit established using a time-delocalized description of the Lugano process, known as the Lugano circuit. The central research question focuses on understanding how the ability of the Lugano process to achieve the LOCC Shift basis measurement protocol manifests itself in the Lugano circuit.

Unitaries inspired by the protocol are devised and incorporated into the Lugano circuit, resulting in a circuit which exhibits interesting properties that enable a complete measurement of the Shift basis. A LOCC protocol is established using this result, allowing for the distinction of the first six Shift states and the detection of the presence of the last two without distinguishing between them.

To gain further insights, the Lugano circuit is converted into an acausal circuit using time-delocalized subsystems, where the conceived unitaries are inserted. This computation aims to identify the fundamental step that corresponds to the trade-off between complete distinguishability under LOCC and indefinite causal order.

Overall, this thesis contributes to the understanding of the relationship between indefinite causal structure and QNWE. A notable further investigation suggested is to pursue the computation into the acausal circuit and analyze its capabilities.

**Keywords:** Process matrix, indefinite causal structure, Lugano process, time-delocalized subsystems, quantum nonlocality without entanglement, Shift basis.

## *Acknowledgements*

I would like to first thank my thesis supervisor Ognyan Oreshkov, and my thesis co-supervisors Julian Wechs and Ravi Kunjwal, for giving me the opportunity to complete this master's thesis. With my engineering background I never anticipated the opportunity to immerse myself in a subject as captivating and as far in theoretical physics as quantum causality. They dedicated their time to guide me, answer my questions, and to show me the valuable thought processes of a theoretical physicist.

Thank in particular to Julian who dedicated a lot of time in clarifying complex concepts and for sharing climbing sessions, which served as refreshing study break.

En deuxième lieu, j'aimerais remercier ma maman qui a toujours été inconditionnellement supportive et présente pour moi. Elle est un élément essentiel qui a contribué à façonner la personne que je suis.

Ensuite, j'aimerais remercier mes amis avec qui j'ai partagé ces cinq années d'études. Je suis reconnaissant d'avoir des amis comme vous à mes côtés, on a vécu pas mal de bons moments ensemble et j'espère que nous continuerons à en avoir tout au long de nos vies. Je suis impatient de découvrir ce que l'avenir nous réserve.

En particulier, je tiens à exprimer ma gratitude spontanément et sans préférence particulière à :

- La Cooloc pour cette année passée ensemble, qui m'a permis de prendre mon indépendance et de m'avoir offert un environnement de vie aussi agréable.
- François pour avoir été mon premier ami en Polytech et pour l'être resté tout du long.
- Alexis pour ta camaraderie, ton humour et l'idée du Neithercircuit.
- Oliver pour ta constante bonne humeur, les spaghettis midi et ta manière de penser originale.
- Xiao-Long pour toutes les aventures qu'on a vécues ensemble qui m'ont permis de sortir ponctuellement de la bulle Polytech.
- Khalil pour avoir été mon partenaire d'étude durant toutes ces journées passées en bibli.
- Batou pour la Figure 7.2 et pour nos weekends de retraite à Transinne.
- Zerpy pour tes blagues, ta French touch et de nous avoir fait découvrir la culture lilloise et le carnaval de Bergues.

Et à tous les autres, papa pour ton soutien, Thibaut pour nos moments musicaux, Eva pour être ma bestie d'escalade, Victor pour ta tente, Jeanne pour tous les blindtests, Thomas pour nos sorties sportives, Yang pour nos sorties bouffes, Suzanne pour les bons moments à Fontainebleau et à la Foscup, Robin pour notre première année d'étude très skerk, Guillaume pour ton support belgo-franco-suisse, et bien sûr je souhaite remercier le reste de ma famille.

# Contents

<b>Abstract</b>	<b>i</b>
<b>Acknowledgements</b>	<b>ii</b>
<b>1 Introduction</b>	<b>1</b>
1.1 Context	1
1.2 Scope of the Thesis	2
1.3 Structure of the Thesis	3
<b>I Theoretical Framework</b>	<b>4</b>
<b>2 Key Concepts of Quantum Theory</b>	<b>5</b>
2.1 Hilbert space and state vector	5
2.2 Inner product, Norm and Outer Product	6
2.3 Liouville Space and Density Operator	7
2.3.1 Pure States, Mixed States and Density Operator	7
2.4 Unitary Operation	7
2.5 Measurement	8
2.5.1 General Measurement	8
2.5.2 Projective Measurement	8
2.5.3 POVM (Positive Operator-Valued Measure)	9
2.6 Quantum Operation	9
2.6.1 Stinespring Dilation Theorem	10
2.7 Quantum Circuit	10
2.7.1 NOT Gate	10
2.7.2 CNOT Gate	11
2.7.3 Hadamard Gate	11
2.7.4 SWAP Gate	12
<b>3 Modelling Indefinite Causal Structure</b>	<b>13</b>
3.1 Process Matrix Formalism	13
3.1.1 Example of a Causally Indefinite Process: The Quantum Switch	14
3.1.2 Quantum Instrument	15
3.1.3 CJ Isomorphism	16
Pure CJ Isomorphism	16
Mixed CJ Isomorphism	16
3.1.4 Link Product	16
3.1.5 Process Matrix	17
3.2 Unitary Extension of the Process Matrix	18
3.3 Time-delocalized Subsystems	19
3.3.1 Generalization to the Tripartite Case	20

<b>4</b>	<b>Quantum Nonlocality Without Entanglement and Lugano Process</b>	<b>23</b>
4.1	Local Operation and Classical Communication (LOCC)	23
4.2	Quantum Nonlocality Without Entanglement	23
4.2.1	Shift Basis	23
4.3	Lugano Process	24
4.4	Lugano process-based LOCC Shift Basis Measurement (LLSBM)	25
4.4.1	Quantum Circuit Generating the Shift Basis	26
<b>II</b>	<b>Results</b>	<b>27</b>
<b>5</b>	<b>Lugano Process Implementation by the Lugano Circuit</b>	<b>28</b>
5.1	Total Unitary of the Lugano Circuit	29
5.2	Unitary Transformation resulting from the Unitary Extension of the Lugano Process	29
5.3	Equality of Differing Terms	32
<b>6</b>	<b>Shift States Distinguishability of the Lugano Circuit</b>	<b>34</b>
6.1	Design of the Unitaries	34
6.2	Implementation of the Unitaries in the Lugano Circuit	35
6.3	Shift Basis Measurement of the Niedercircuit	37
6.3.1	Shift State $ 000\rangle$	37
6.3.2	Shift State $ 111\rangle$	37
6.3.3	Shift State $ +01\rangle$	38
6.3.4	Shift State $ -01\rangle$	38
6.3.5	Shift States $ 1+0\rangle$ and $ 1-0\rangle$	38
6.3.6	Shift States $ 01+\rangle$ and $ 01-\rangle$	38
6.3.7	Summary	38
6.4	LOCC Protocol to Distinguish the Shift Basis	39
6.4.1	LOCC Protocol for the six First Shift states	39
	First step	39
	Second step if Charlie communicates 0	39
	Second step if Charlie communicates 1	40
6.4.2	Protocol on the last two Shift states	41
	Charlie communicates 0	41
	Charlie communicates 1	41
	Summary	41
<b>7</b>	<b>Description of the Lugano Circuit in the Process Matrix Formalism</b>	<b>43</b>
7.1	$R(U_C)$ computation	43
7.1.1	$( U_1^\dagger\rangle\rangle_{C_I Z P_O A B O} * ( I\rangle\rangle_{A_O \bar{T}_1} \otimes  I\rangle\rangle_{B_O \bar{T}_2})$ computation	44
7.1.2	$(( I\rangle\rangle_{\bar{T}_1 B_I} \otimes  I\rangle\rangle_{\bar{T}_2 A_I}) *  U_2^\dagger\rangle\rangle_{A B_I F_I C_O \bar{Z}})$ computation	45
7.1.3	$ \omega_1(U_C)\rangle\rangle$ computation	45
7.1.4	$ \omega_2^\circ(U_C)\rangle\rangle$ and $ \omega_2^\bullet(U_C)\rangle\rangle$ computation	45
7.1.5	$ \omega_3(U_C)\rangle\rangle$ computation	46
7.1.6	Vectors Composition	46
	First composition	46
	Third composition	47
	Fourth composition	47
	Fifth composition	48
7.1.7	Final Result	48

<b>8 Conclusion and Further Investigations</b>	<b>50</b>
<b>A Appendices to Chapter 1</b>	<b>51</b>
A.1 Spacetime Interval between two Events . . . . .	51
<b>B Appendices to Chapter 2</b>	<b>53</b>
B.1 Linear Operator . . . . .	53
B.2 Trace . . . . .	54
B.2.1 Partial trace . . . . .	54
<b>C Appendices to Chapter 5</b>	<b>55</b>
C.1 Numerical Computation of the Total Unitary of the Lugano Circuit . . . . .	55
<b>Bibliography</b>	<b>57</b>

# Notation Conventions

$H$	Hilbert space
$H^X$	Hilbert space with label $X$
$\{ i\rangle\}$	Orthonormal basis in a specified Hilbert space
$d_X$	Dimension of the Hilbert space $H^X$
$I_X$	Identity on $H^X$
$H^{XY} = H^X \otimes H^Y$	Tensor product of the Hilbert spaces $H^X$ and $H^Y$
$L(H^X)$	Liouville space of operators acting in $H^X$
$L(H^X, H^Y)$	Liouville space of operators acting from $H^X$ to $H^Y$
$L(L(H^X), L(H^Y))$	Liouville space of operators acting in $H^X$ to operators acting in $H^Y$
$A \prec B$	Event A causally precedes event B
$A_I$ and $A_O$	Labels for respectively the ingoing and outgoing system of party A
$AB_{IO}$	Label for the tensor product of the ingoing and outgoing systems of parties A and B
$ I\rangle\rangle = \sum_i  i\rangle \otimes  i\rangle$	Maximally entangled state
$\oplus$	Modulo 2 addition

# List of Abbreviations

<b>CJ</b>	<b>Choi-Jamiołkowski</b> (Chapter 3.1.3)
<b>CP</b>	<b>Completely Positive</b> (Chapter 2.6)
<b>CPTP</b>	<b>Completely Positive Trace-Preserving</b> (Chapter 2.6)
<b>LLSBM</b>	<b>Lugano process-based LOCC Shift Basis Measurement</b> (Chapter 4.4)
<b>LOCC</b>	<b>Local Operations (and) Classical Communication</b> (Chapter 4.1)
<b>QNWE</b>	<b>Quantum Nonlocality Without Entanglement</b> (Chapter 4.2)
<b>QT</b>	<b>Quantum Theory</b> (Chapter 2)
<b>TDS</b>	<b>Time-Delocalized quantum Subsystems</b> (Chapter 3.3)
<b>TP</b>	<b>Trace-Preserving</b> (Chapter 2.6)



## Chapter 1

# Introduction

### 1.1 Context

**Causality** is a fundamental concept in physics; an event A causing an event B must precede it in time. All fundamental theories of physics assume a definite order of event and allow to say without ambiguity if A is in the causal past of B, the opposite or the two are space-like separated.<sup>1</sup>

However, the quest for the unification of **quantum theory (QT)** with **general relativity** into a theory of **quantum gravity** has led to a rethinking of the causal structure of quantum mechanics. The reason is that on the one hand, QT is a *probabilistic* theory with a **fixed** causal structure, that is, the causal structure is always everywhere well-defined. But on the other hand, general relativity is a *deterministic* theory with a **dynamic** causal structure, that is, the mass distribution creates a local spacetime bending that affects the causal structure by deforming the light cone.

With these two things in mind, one can speculate that quantum gravity would be a probabilistic theory with a dynamic causal structure. [21]

Several frameworks that revisit the causal structure of quantum mechanics currently exist [29, 21, 25, 5]. These ideas form the area of research that is **quantum causality**, which is a relatively new and rapidly growing field.

The framework considered in this thesis is the **process matrix formalism** first introduced in [29]. It allows to describe the most general causal relationships possible between local parties, performing operations described by standard QT, without creating logical paradoxes. This gives rise to situations where the causal order between these parties is **indefinite**.<sup>2</sup>

Aside from the above foundational incentive, there are benefits to drop the assumption of a definite causal structure such as the violation of causal inequalities [29] and other informational tasks otherwise impossible [10, 1, 18, 15]. These applications are all the more interesting knowing that a causally indefinite process, the **quantum switch**, has been realized experimentally [30, 31, 17] and has already been used to obtain computational advantages [36, 19].

The experimental realization of the quantum switch has given rise to debate whether it consists in a genuine physical implementation of a process with indefinite causal structure or only a simulation of it. To address this question and gain a better understanding of the experiment, the concept of **time-delocalized quantum subsystems (TDS)** has recently

---

<sup>1</sup> For a reader unfamiliar with these concepts, some insights into the concepts of causal relationships between events in spacetime and light cone are developed in Appendix A.

<sup>2</sup> This formalism is presented in more details in Chapter 3.1.

been introduced in [28]. This concept consists of changing how quantum circuit operations are described, shifting from acting on subsystems with definite time to subsystems that are not associated with specific times.<sup>3</sup> This initially allowed to establish a correspondence between all **unitarily extensible** bipartite processes<sup>4</sup>, even those with an indefinite causal order, and temporally ordered quantum circuit from standard QT.

Last year, it was proved in [34] that this correspondence can be generalized to all unitarily extensible tripartite processes together with their unitary extensions. The same paper then use this result to obtain a temporally ordered circuit of a known unitarily extensible tripartite causally indefinite classical process, the **Lugano process**. [7]

A feature of interest of the Lugano process is that it was shown in [24] that it allows to perform another impossible task assuming a well-defined causal order: the perfect distinguishability of, a set of separable and orthogonal three-qubits states known as, the **Shift basis** through **local operation and classical communication (LOCC)**. This is something which should not be possible because of **quantum nonlocality without entanglement (QNWE)**, as first shown in [8], but is realizable at the cost of losing a definite causal structure.<sup>5</sup> For readability, this measurement protocol is named the **Lugano LOCC Shift basis measurement (LLSBM)**.

With this context in mind, one could wonder what happens if we take the LLSBM and try to implement it within a temporally ordered circuit that executes the Lugano process. How would this circuit behave ? How much of Shift basis distinguishability would it offer ? What are its characteristics of QNWE under LOCC ? Using TDS, there is a correspondence between the circuit and the process matrix representation of the Lugano process. At which step of this correspondence would the trade between QNWE and causal order takes place ?

These are the questions that motivate this thesis.

## 1.2 Scope of the Thesis

The central research question that this thesis follows is "*How does the ability of the causally indefinite Lugano process to achieve the Shift basis measurement with LOCC manifest itself in its implementation into a temporally ordered circuit ?*".

To answer this question, we work with a simplified version of the temporally ordered circuit, named the **Lugano circuit**, established by J. Wechs [33]. We begin by showing that this simplified circuit indeed implements the Lugano process expressed in the process matrix formalism.

We then devise unitaries that are the dilations of the specific operations performed by the parties in the LLSBM. By incorporating these unitaries into the Lugano circuit, we observe that it successfully implements the Shift basis measurement. This result in a circuit, with unique properties, which are analyzed to better understand the capabilities of the circuit in terms of Shift basis measurement. Through this analysis, a LOCC protocol is established that allows an almost complete Shift basis measurement by allowing to

3 The notion of TDS is presented in more details in Chapter 3.3.

4 More precisely, all unitarily extensible bipartite processes together with their unitary extensions, of which the quantum switch is an example. The notion of unitary dilation is explained in Chapter 2.6.1 and the one of unitarily extensible process in Chapter 3.2.

5 The concepts of QNWE, Shift basis and LOCC are presented in Chapter 4.

distinguish the six first Shift states and to know if we are in the presence of the last two without being able to distinguish them.

We discuss that it's still unclear how the Shift states can be completely distinguished when transitioning from a temporally ordered circuit to an acausal one. To gain further insight into this issue, a detailed computation was conducted on the non-simplified Lugano circuit to convert it into an acausal circuit using the process matrix formalism with conceived unitaries. This computation we hope will allow to identify the trade-off between complete distinguishability under LOCC and indefinite causal order.

### 1.3 Structure of the Thesis

This thesis consists of two parts. The first part establishes the theoretical framework necessary for comprehending the thesis:

- Chapter 2, provides a review of relevant notions of QT.
- Chapter 3, introduces key concepts related to modeling an indefinite causal structure, including the process matrix formalism, TDS and the quantum switch.
- Chapter 4, presents the elements related to the Shift basis measurement protocol such as QNWE and the Lugano process.

The second part contains the results of this thesis, along with their corresponding analyses and discussions:

- Chapter 5, demonstrates the equivalence of the Lugano circuit with the Lugano process expressed in the process matrix formalism.
- Chapter 6, presents the unitary and the circuit developed, performs an analysis of their properties and establish a LOCC protocol allowing an almost complete distinguishability of the Shift states.
- Chapter 7, examines the correspondence from the non-simplified Lugano circuit, with conceived unitaries, to an acausal circuit.
- Chapter 8, finishes the thesis with a conclusion and considerations for further investigations.

## **Part I**

# **Theoretical Framework**

## Chapter 2

# Key Concepts of Quantum Theory

**Quantum theory (QT)** is the theory that describes the behavior of matter and energy at small scales. It introduces a set of rules, concepts and notations allowing to successfully model quantum physical systems. This enables to study the temporal evolution of these systems, to perform measurements on them and to analyze their particularities. This theory has been around for a long time, but recent advances have been made in the sub-branch of **quantum information**.

Quantum information investigates how quantum systems can be used to treat information by exploiting quantum properties, such as superposition and entanglement, to perform certain tasks more efficiently than what is possible using classical methods.

This chapter introduces some key concepts of quantum theory and quantum information relevant for this thesis. It assumes the reader to be comfortable with linear algebra. Parts of this chapter are based on Chapter 2 of [26] and first part of [22].

## 2.1 Hilbert space and state vector

Any isolated physical system is associated to a **Hilbert space** (denoted by  $H$ ) which is a complex vector space with inner product. All vectors of unit norm of the Hilbert space correspond to all the potential states in which the system could be. We call such a vector a **state vector**, a given state of the system is completely described by it.

In this thesis, we work only with finite dimensional Hilbert spaces as we do not consider instances where it is relevant to switch to the continuous case.

Quantum theory uses a particular notation for vectors called the **bra-ket notation**, it allows to efficiently represent the algebraic operations performed between the Hilbert space and its **dual space** (denoted by  $H^*$ ). In this notation, a state vector or "ket" is written

$$|\psi\rangle \in H$$

while the dual of the state vector or "bra" is obtained by taking its adjoint  $\dagger$ , which corresponds to his conjugate transpose.

$$|\psi\rangle^\dagger = \langle\psi| \in H^*$$

A state vector has a **matrix representation** for a given basis. It is a column vector whose elements are the components of the vector in this specific basis,

$$|\psi\rangle = \begin{bmatrix} \psi_1 \\ \psi_2 \\ \vdots \\ \psi_n \end{bmatrix}_{(n \times 1)}$$

where  $|\psi\rangle$  belongs to a Hilbert space of dimension  $n$  and whose components  $\psi_i$  are complex numbers.

The matrix representation of the corresponding dual vector is

$$\langle\psi| = \begin{bmatrix} \psi_1^* & \psi_2^* & \cdots & \psi_n^* \end{bmatrix}_{(1 \times n)}$$

Another way of representing the state vectors is in terms of a linear combination of a basis. Let  $\{|i\rangle\}$  be an orthonormal basis in  $H$ , we can decompose

$$|\psi\rangle = \sum_i \psi_i |i\rangle$$

An important concept in quantum information is the **qubit** (abbreviation for quantum bit) which is mathematically described by a state vector in a two-dimensional Hilbert space. A qubit is most often described in the **computational basis**  $\{|0\rangle, |1\rangle\}$

$$|\psi\rangle = \alpha|0\rangle + \beta|1\rangle = \alpha \begin{bmatrix} 0 \\ 1 \end{bmatrix} + \beta \begin{bmatrix} 1 \\ 0 \end{bmatrix} = \begin{bmatrix} \alpha \\ \beta \end{bmatrix}$$

Where  $\alpha$  and  $\beta$  are complex numbers with  $|\alpha|^2 + |\beta|^2 = 1$  for normalization.

Common concrete examples of qubits are photons in superposition of horizontal and vertical polarization states or particles in superposition of spin states.

## 2.2 Inner product, Norm and Outer Product

Each dual vector  $\langle\phi| \in H^*$  is a **linear operator** that sends a vector  $|\psi\rangle \in H$  to a complex number.<sup>1</sup> This operation is called the **inner product** and is written  $\langle\phi|\psi\rangle$ . Two vectors are orthogonal to each other if their inner product is zero.

The inner product allows to define the **norm** of a vector in a Hilbert space. It is given by  $\| |\psi\rangle \| = \sqrt{\langle\psi|\psi\rangle}$ .

Two vectors of a Hilbert space can be used to define an **outer product**  $|\psi\rangle\langle\phi|$  whose action on an arbitrary vector  $|\varphi\rangle$  of the same Hilbert space is given by

$$(|\psi\rangle\langle\phi|)|\varphi\rangle = \langle\phi|\varphi\rangle|\psi\rangle$$

The outer product allows to demonstrate the **completeness relation**.

$$\left( \sum_i |i\rangle\langle i| \right) |\psi\rangle = \sum_i |i\rangle\langle i|\psi\rangle = \sum_i \psi_i |i\rangle = |\psi\rangle$$

Since this equation is true for all  $|\psi\rangle$ , it follows that  $\sum_i |i\rangle\langle i| = I$  where  $I$  is the identity operator.

<sup>1</sup> The notion of linear operators is explained in Appendix B.1.

## 2.3 Liouville Space and Density Operator

One important concept rising from the one of Hilbert space is the associated **Liouville space** (denoted by  $L(H)$ ). It is the space of linear operators that act on  $H$ . The Liouville space is also a Hilbert space but with a different inner product known as the **Hilbert-Schmidt inner product**.

For two operators  $A, B \in L(H)$ , this inner product is defined as  $(A, B) = \text{tr}(A^\dagger B)$ .<sup>2</sup>

The Liouville space can be understood as equivalent to the tensor product of a Hilbert space with its dual.

The description of physical systems in term of state vectors in Hilbert space can be generalized to **density operator**<sup>3</sup> in Liouville space.

### 2.3.1 Pure States, Mixed States and Density Operator

The state of a quantum system can be either **pure** or **mixed**. A pure state is one for which we have complete information about the system, in the sense that there is no classical uncertainty regarding the quantum state, and we can describe the system using a single state vector  $|\psi\rangle$ . [20]

On the other hand, a mixed state is one for which we have incomplete information about the system. In this case, we resort to (classical) statistics to describe the state. Suppose that we have a quantum system which is in one of a number of states  $|\psi_i\rangle$ , with respective probabilities  $p_i$ . We write the ensemble of pure states  $\{p_i, |\psi_i\rangle\}$  and the density operator for this system [26]

$$\rho = \sum_i p_i |\psi_i\rangle \langle \psi_i|$$

In order for the density operator to be a physical state, it must be Hermitian positive semi-definite to ensure that the probabilities  $p_i$  associated with the eigenvalues are nonnegative. And its trace must be equal to one such that the probabilities  $p_i$  sum up to one.

## 2.4 Unitary Operation

The evolution of a closed quantum system is described by unitary operators. A unitary operator, denoted  $U$ , acts on a quantum state  $|\psi\rangle$  and produces a new state  $|\psi'\rangle$  according to

$$|\psi'\rangle = U|\psi\rangle$$

The important property of unitary operator is that their transpose conjugate is equal to their inverse

$$U^\dagger = U^{-1}$$

This ensures that the normalization of the state vector is preserved. To illustrate this, let's take the inner product of the evolved state vector

$$\langle \psi | U^\dagger U | \psi \rangle = \langle \psi | U^{-1} U | \psi \rangle = \langle \psi | \psi \rangle = 1$$

Additionally, this property guarantees that unitary operators are reversible. By taking the inverse of a unitary operator, we can revert the evolution and recover the original state.

<sup>2</sup> The notion of trace and partial trace is explained in Appendix B.2.

<sup>3</sup> also called **density matrix** when referring at its matrix representation.

System evolution can also be described with density operators, for example the unitary evolution of a density operator  $\rho$  is given by

$$\rho' = U\rho U^\dagger$$

## 2.5 Measurement

Doing a measurement on a quantum system changes it. This corresponds to lose information on its statistical properties, by extracting a value into the macroscopic world. This can be represented mathematically by different types of measurements that we introduce here.

### 2.5.1 General Measurement

A measurement on a quantum system gives one of a discrete set of possible values. A way of representing it is by using a set of operators, each corresponding to a possible result, acting on the state space of the system being measured.

These **measurement operators** are denoted  $\{M_m\}$  where  $m$  is an index that refers to the possible measurement outcomes. The probability that an outcome  $m$  occurs after a measurement on state  $|\psi\rangle$  is given by

$$p(m) = \langle\psi|M_m^\dagger M_m|\psi\rangle$$

Since the probabilities sum to one, the measurement operators must obey the completeness relation

$$\sum_m p(m) = 1 \quad \longrightarrow \quad \sum_m M_m^\dagger M_m = I$$

The new state of the system after a measurement with result  $m$  is

$$|\psi_m\rangle = \frac{M_m|\psi\rangle}{\sqrt{\langle\psi|M_m^\dagger M_m|\psi\rangle}}$$

In terms of density operator, the probability that the outcome  $m$  occurs is  $p(m) = \text{tr}(M_m\rho)$  and the post-measurement state is

$$\rho_m = \frac{M_m\rho M_m^\dagger}{\text{tr}(M_m^\dagger M_m\rho)}$$

The density operator enables to capture the different possible measurement outcomes while accounting for the classical uncertainty of the system.

### 2.5.2 Projective Measurement

Another common way of formulating measurements in QT is **projective measurements**. It consists in a special case of general measurements where the measurement operators  $M_m$ , now called **projective operators**, are Hermitian, orthogonal and idempotent.

In this case,

$$p(m) = \langle\psi|M_m^\dagger M_m|\psi\rangle = \langle\psi|M_m^2|\psi\rangle = \langle\psi|M_m|\psi\rangle$$



The measurement is described by an observable  $O$ , which is an Hermitian operator which can always be described as a spectral decomposition of projective operators  $O = \sum_m m M_m$  whose eigenvalues are the possible measurement results.

The new state of the system, after a projective measurement of result  $m$  is

$$|\psi_m\rangle = \frac{M_m|\psi\rangle}{\sqrt{\langle\psi|M_m|\psi\rangle}}$$

Projective measurement has the valuable property that the average value of the observable  $\langle O \rangle$  is

$$\langle O \rangle = \sum_m m p(m) = \sum_m m \langle\psi|M_m|\psi\rangle = \langle\psi|(\sum_m m M_m)|\psi\rangle = \langle\psi|O|\psi\rangle$$

### 2.5.3 POVM (Positive Operator-Valued Measure)

In some cases, the interest of a measurement is in the probabilities of its respective outcomes and not in the post-measurement state of the system. The **POVM formalism** is used for these applications.

From the set of measurement operators  $\{M_m\}$ , we can define a set of **POVM elements**  $\{E_m = M_m^\dagger M_m\}$ . Which are positive operators (their eigenvalues are nonnegative) that satisfy  $\sum_m E_m = I$

The set of operators  $E_m$  are sufficient to determine the probabilities of the different measurement outcomes.

$$p(m) = \text{tr}(E_m \rho) = \sum_i \langle i|E_m|\psi\rangle \langle\psi|i\rangle = \sum_i \langle\psi|i\rangle \underbrace{\langle i|E_m|\psi\rangle}_I = \langle\psi|E_m|\psi\rangle$$

## 2.6 Quantum Operation

As we have seen, unitaries allow to describe physically realisable transformations on closed quantum systems. However, when dealing with open systems, we need a more general framework known as **quantum operations**. Quantum operations, also referred to as **quantum channels** or **quantum processes**, are linear maps that act on Liouville spaces. They allow us to describe physically realizable transformations on open systems.

We note such a quantum operation  $\mathcal{E}(\rho) : \rho \rightarrow \mathcal{E}(\rho)$ .

To ensure that the quantum operations describe physically meaningful evolutions, they must satisfy certain requirements. Firstly, they must be positive, meaning that the probabilities associated with the outcomes of measurements are nonnegative. Secondly, quantum operations must be **trace-preserving (TP)**

$$\text{tr}(\mathcal{E}(\rho)) = \text{tr}(\rho) = 1 \forall \rho$$

This ensures that the probabilities of the output density operator  $\rho'$  all sum up to one.

Merely being positive is not sufficient; we also require **complete positivity (CP)** for quantum operations. It ensures that even when the operation is extended to act on a part of a larger system, it remains positive. This condition is crucial to treat open system where an outside system can have influence on the operation.

In summary a quantum operator must be a linear **completely positive trace-preserving (CPTP)** map.

### 2.6.1 Stinespring Dilation Theorem

We presented two approaches to model the dynamics of a quantum system: using unitary operations for closed system or CPTP maps for open system. While these models may seem disconnected, a correspondence between them can be established through the **Stinespring dilation theorem**.<sup>4</sup>

This theorem states that if the evolution of a density operator is described by a CPTP map, there exists a corresponding unitary operation acting on a larger Hilbert space. This larger system includes the original system of interest as well as an ancillary system.

By applying this unitary evolution on the joint system and subsequently tracing out the ancillary system, we can retrieve the evolution described by the CPTP map on the original system. In other words, any quantum channel, represented by a CPTP map, can be derived from an initial unitary operation acting on a larger system.

## 2.7 Quantum Circuit

The **Quantum circuit** model is a valuable model used in the field of quantum information to represent operations that a quantum system undergoes. In this model, quantum systems evolve through a sequence of **quantum logical gates**, quantum channels and measurements.

In the following sections, we will introduce some of the essential quantum gates employed in this thesis. It is important to note that these gates manipulate qubits, which are the quantum counterparts of classical bits. A gate operates on inputs comprising one or multiple qubits. Unlike classical gates, quantum gates are always reversible as they involve unitary transformations.

### 2.7.1 NOT Gate

The NOT gate, also known as the Pauli X gate, is a basic quantum logic gate that operates on a single qubit. It works by flipping the state of the qubit, changing  $|0\rangle$  to  $|1\rangle$  and vice versa.



FIGURE 2.1: Representation of the NOT gate in quantum circuit.

Mathematically, the NOT gate corresponds to the application of the Pauli X unitary which matrix representation in the computational basis is

$$X = \begin{bmatrix} 0 & 1 \\ 1 & 0 \end{bmatrix}$$

<sup>4</sup> More information on this theorem can be found in the paper that first introduced it [32].

### 2.7.2 CNOT Gate

The CNOT (Controlled-NOT) gate operates on two qubits: a control qubit and a target qubit. The control qubit remains unchanged, while the target qubit undergoes a NOT operation if the control qubit is in state  $|1\rangle$ .

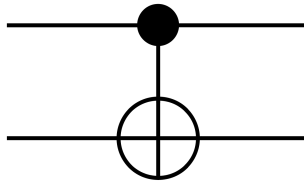


FIGURE 2.2: Representation of the CNOT gate in quantum circuit.

The working of the CNOT can be modeled as the operation  $|0\rangle\langle 0| \otimes I + |1\rangle\langle 1| \otimes X$

When the control black dot is replaced by a white circle, this means that the controlled gate has the opposite working : the gate is performed when the control qubit is in state  $|0\rangle$ .

The CNOT gate can be generalized to a three-qubit system as the Toffoli gate. The Toffoli gate operates on two control qubits and a target qubit. It applies a logical NOT operation to the target qubit only if both control qubits are in the state  $|1\rangle$ .

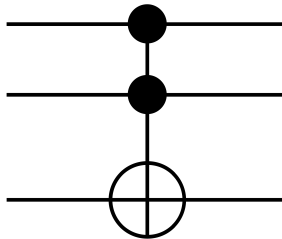


FIGURE 2.3: Representation of the Toffoli gate in quantum circuit.

It can be modeled as the operation

$$(|0\rangle\langle 0| \otimes |0\rangle\langle 0| + |0\rangle\langle 0| \otimes |1\rangle\langle 1| + |1\rangle\langle 1| \otimes |0\rangle\langle 0|) \otimes I + |1\rangle\langle 1| \otimes |1\rangle\langle 1| \otimes X$$

### 2.7.3 Hadamard Gate

The Hadamard gate is a single-qubit gate that allows to get superposed states from state of the computational basis and vice-versa.

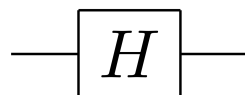


FIGURE 2.4: Representation of the Hadamard gate in quantum circuit.

It works in the following way

Input	Output
$ 0\rangle$	$ +\rangle$
$ 1\rangle$	$ -\rangle$
$ +\rangle$	$ 0\rangle$
$ -\rangle$	$ 1\rangle$

where  $|\pm\rangle$  stands for  $\frac{1}{\sqrt{2}}(|0\rangle \pm |1\rangle)$ .

And the corresponding unitary in the computational basis is  $H = \frac{1}{\sqrt{2}} \begin{bmatrix} 1 & 1 \\ 1 & -1 \end{bmatrix}$ .

#### 2.7.4 SWAP Gate

The SWAP gate is a two-qubit gate that exchanges the states of two qubits.

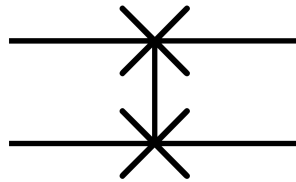


FIGURE 2.5: Representation of the SWAP gate in quantum circuit.

It can be modeled as the operation

$$|0\rangle\langle 0| \otimes |0\rangle\langle 0| + |0\rangle\langle 1| \otimes |1\rangle\langle 0| + |1\rangle\langle 0| \otimes |0\rangle\langle 1| + |1\rangle\langle 1| \otimes |1\rangle\langle 1|$$

## Chapter 3

# Modelling Indefinite Causal Structure

A physical process with an **indefinite causal structure** refers to a scenario in which multiple **parties** locally perform quantum operations, but it is not possible to establish a well-defined causal ordering of these operations. The **process matrix formalism** employed to describe such processes allows for general situations where parties can base their operations depending on their input systems, resulting in output systems that can subsequently influence the operations performed by other parties while maintaining an indefinite causal order of the parties' operations and without creating logical paradoxes. While this may seem counterintuitive to our perceptions, an implementation of such a process, known as the **quantum switch**, has been experimentally realized [30, 31, 17] and has already been used to obtain computational advantages [36, 19] unreachable in situations with well-defined causal order. Furthermore, a description of QT lacking a definite causal structure could potentially have relevance for quantum gravity. [21, 29]

This chapter presents the framework used in this thesis to model causally indefinite processes.

### 3.1 Process Matrix Formalism

The process matrix formalism considers multiple parties (usually named Alice, Bob, Charlie, etc.), each of whom interacts with an input quantum system and produces an output quantum system, without a definite causal order between them.

More precisely, each party is assumed to be in its **closed** laboratory, in the sense that it is completely isolated from the outside world during its operations. The laboratory is opened only for the entry and exit of the system, and is otherwise kept closed between these events. [29]

The **process matrix**  $W$  serves as a mean to connect local operations and determine their causal relationship, whether definite or indefinite. Essentially, it takes into account all physical processes occurring outside of the local laboratories. This allows for the complete determination of the outcome probabilities of the process based on the chosen local operations and the way the process matrix connects the laboratories. [9]

This formalism is the most general possible, allowing for the description of a wide range of causal structures. The only constraint is that it must lead to valid outcome probabilities. However, this generality leads to the existence of processes where it is unclear whether they have a physical interpretation or realization and makes the formalism more complex to understand.

To provide a preliminary understanding of the concept, we will first present an example of a causally indefinite process: the quantum switch. The quantum switch can be interpreted in a physical way as a controlled superposition of two causal orders. This example offers some intuition about the formalism before delving into its mathematical description.

### 3.1.1 Example of a Causally Indefinite Process: The Quantum Switch

The **quantum switch** is a causally indefinite bipartite process involving Alice and Bob (denoted by A and B). It involves a two-qubit state consisting of a control and a target qubit (respectively denoted by  $|t\rangle$  and  $|c\rangle$ ).

The local operations performed by A and B on the target qubit  $|t\rangle$ . The two parties A and B apply their local operation on  $|t\rangle$  depend on the state of the control qubit  $|c\rangle$ . If  $|c\rangle = |0\rangle$ , A acts before B. Conversely, if  $|c\rangle = |1\rangle$ , B acts before A.

The interesting aspect of the quantum switch arises when the control qubit is put in a superposition state, for example,  $|c\rangle = |+\rangle$ . In this case, the operations performed by A and B are applied to the target qubit in a superposition of orders, resulting in an indefinite causal structure where both  $A \prec B$  and  $B \prec A$ . Such a process cannot be described by standard quantum theory (QT) and requires the use of the process matrix formalism.

Figure 3.1 illustrates the causal orders in the quantum switch process for both  $|c\rangle = |1\rangle$  and  $|c\rangle = |+\rangle$ , where  $|t\rangle^{in}$  and  $|t\rangle^{out}$  represent the state of the target qubit before and after the quantum switch operation, respectively.

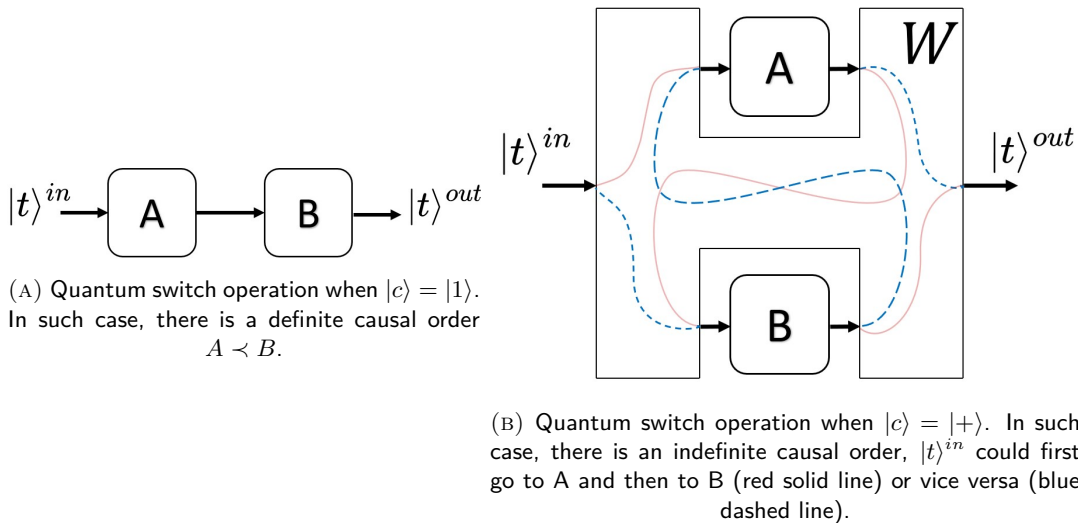


FIGURE 3.1: Illustration of the quantum switch causal order for two different values of the control qubit.

The quantum switch, which was first introduced in [11], has since been experimentally realised in multiple laboratory, as documented in notable studies such as [30, 31, 17]. One example of its implementation is an optical setup using a photon emitter. In this setup, a beamsplitter coherently controls the order of the two operations by selectively transmitting or reflecting the incident photon based on its polarization state.

Before describing mathematically the process matrix formalism, it is necessary to introduce several mathematical notions, starting with the one of **quantum instrument**.

### 3.1.2 Quantum Instrument

Quantum channel describes the most general evolution that a quantum state can undergo. However, for the process matrix formalism, we need to consider what are the measurement results of each party. We are thus looking for the most general evolution that transforms an input quantum system to both an output quantum system and a classical register that records the corresponding measurement outcome. Such evolution is given by a **quantum instrument**. [14]

Mathematically, a quantum instrument  $\{\mathcal{M}_m\}$  is a set of CP trace non-increasing maps  $\mathcal{M}_m$  whose sum  $\sum_m \mathcal{M}_m$  is a CPTP map, where  $m$  labels outcomes of the quantum instrument. In addition, one can consider scenarios where the parties can choose between different quantum instruments based on classical random variables (such as flipping a coin), such classical variables are named the **settings** of the parties.

To illustrate this, let's consider a bipartite process involving Alice and Bob both performing quantum instruments on ingoing and outgoing quantum systems. The incoming quantum systems are labeled by  $A_I$  and  $B_I$ , while the outgoing systems are labeled by  $A_O$  and  $B_O$ , respectively. The laboratories settings are labeled by  $x$  and  $y$ , and  $a$  and  $b$  represent the possible outcomes of their operations. So,  $\mathcal{M}_{a|x}^A \in L(H^{A_I}, H^{A_O})$  represents Alice's instrument for setting  $x$  with outcome  $a$ . This is illustrated in Figure 3.2.

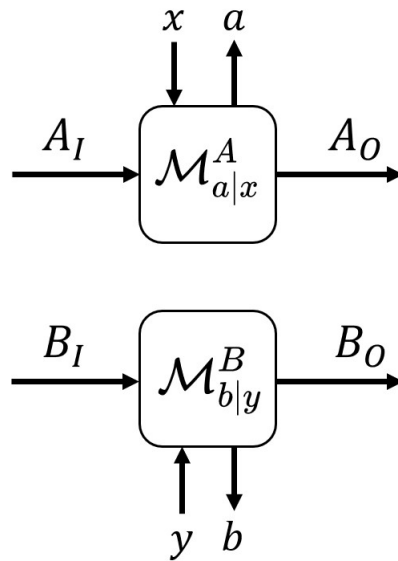


FIGURE 3.2: Illustration of quantum instruments in a bipartite process.

From the definition presented above, one can understand that a singleton quantum instrument is a CPTP map with a single outcome which occurs with certainty. [29]

The notion of quantum instrument will allow to get an expression of the most general correlations that the parties can establish for any causal structure.

However, it is first necessary to introduce some mathematical notions which are the **CJ isomorphism** and the **link product**.

### 3.1.3 CJ Isomorphism

The **Choi-Jamiołkowski isomorphism (CJ isomorphism)** [23, 13] refers to a pair of bijections which are convenient to represent quantum operations and their composition.

### Pure CJ Isomorphism

The **pure** CJ isomorphism establishes a bijection between a linear operator  $A \in L(H^X, H^Y)$  and a vector  $|A\rangle\rangle \in H^{XY}$ . If  $\{|i\rangle\rangle\}$  is an orthonormal basis of  $H^X$  and  $|I\rangle\rangle = \sum_i |i\rangle\rangle \otimes |i\rangle\rangle$  is a maximally entangled state in  $H^{XX}$  then the bijection is given by

$$|A\rangle\rangle = (A \otimes I_X)|I\rangle\rangle = \sum_i A|i\rangle\rangle \otimes |i\rangle\rangle$$

$$A = |A\rangle\rangle^{T_X}$$

where  $T_X$  is the transpose over  $H^X$ .

### Mixed CJ Isomorphism

The **mixed** CJ isomorphism is a bijection between a quantum maps  $\mathcal{M} \in L(L(H^X), L(H^Y))$  and linear operators  $M \in L(H^{XY})$  which is given by

$$M = (\mathcal{M} \otimes I_X)(|I\rangle\rangle\langle\langle I|)$$

$$\mathcal{M}(\rho) = (tr_X(\rho M))^T$$

where  $|I\rangle\rangle\langle\langle I| = \sum_{ij} |i\rangle\rangle\langle\langle j| \otimes |i\rangle\rangle\langle\langle j|$  and  $j$  another label for the basis  $\{|i\rangle\rangle\}$ .

From now on, when referring to quantum operations, we will use the calligraphic font to denote the operators, and the non-calligraphic font to denote their CJ isomorphism.

#### 3.1.4 Link Product

The **link product** is an operation which expresses composition between operators in their CJ representation.

Consider a circuit that successively performs, on an input system, two quantum operators  $\mathcal{M} \in L(L(H^A), L(H^B))$  and  $\mathcal{N} \in L(L(H^B), L(H^C))$ . These two operators can be composed into one  $\mathcal{T} \in L(L(H^A), L(H^C))$ .

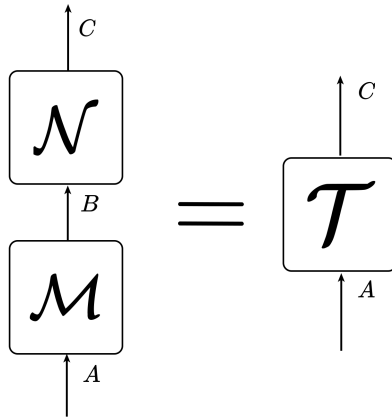


FIGURE 3.3: Composition of two quantum operators.

This can be done through the CJ isomorphism using the link product  $*$  which composes the two into the operator  $T \in L(H^{AC})$ .



$$T = N^{BC} * M^{AB} = \text{tr}_B((N^{BC} \otimes I^A)(I^C \otimes M^{AB}))$$

By taking the link product we get rid of the intermediate spaces of the tensor product of the two quantum operators, that is, we obtain an operator that lives only in the input and output spaces of the circuit.

This link product is extensively use in this thesis, specifically its vector form; Let's consider two vectors  $|a\rangle \in H^{XY}$  and  $|b\rangle \in H^{YZ}$ , their link product is given by

$$|a\rangle * |b\rangle := (I^{XZ} \otimes \langle\langle I^{YY} \rangle\rangle)(|a\rangle \otimes |b\rangle)$$

The action of a linear map  $\mathcal{M}$  on a state  $\rho$  can be rewritten  $\mathcal{M}(\rho) = \mathcal{M} * \rho$ . For a circuit composed of successive linear maps  $\mathcal{M}_1, \mathcal{M}_2, \dots, \mathcal{M}_n$  The circuit output is given by  $\mathcal{M}_1 * \mathcal{M}_2 * \dots * \mathcal{M}_n * \rho$ .

### 3.1.5 Process Matrix

The notion of quantum instrument was used in [29], to get an expression of the most general correlations  $P(a, b|x, y)$  that the parties can establish. These correlations are given by a generalized Born's rule

$$P(a, b|x, y) = \text{tr}(M_{a|x}^{AIO} \otimes M_{b|y}^{BIO} W^{ABIO})$$

Where we use the notation  $ABIO = A_I \otimes A_O \otimes B_I \otimes B_O$  and  $M_{a|x}^{AIO}$  is the CJ form of  $\mathcal{M}_{a|x}^A$ . The **process matrix**  $W^{ABIO}$  is an Hermitian matrix in  $L(H^{ABIO})$  wich can be seen as the environment linking the local operations.

In order for these correlations to be valid probabilities, the process matrix must satisfy certain conditions:<sup>1</sup>

- $W$  must be positive semidefinite to ensure nonnegative correlations.
- $W$  must be normalized:  $\text{tr}(W) = d_{A_O} d_{B_O}$  such that the probabilities sum up to one.
- $W$  must live in a particular linear subspace of  $L(H^{ABIO})$  defined in Appendix B of [4], this ensure that the correlations obtained are constant for any CPTP maps we can plug into the process.

It was demonstrated in [29] that satisfying these conditions implies that the process matrix formalism does not allow for the creation of logical paradoxes, such as scenarios involving an agent going back in time and killing his parents.

For some processes, the process matrix is a rank-one projector  $W = |w\rangle\langle w|$  in such cases, we call the vector  $|w\rangle$  the **process vector**. [4]

Although the process matrix formalism has been presented here for the bipartite case, it can be extended to scenarios involving more than two parties.

<sup>1</sup> More details about these conditions can be found in Appendix B of [4].

## 3.2 Unitary Extension of the Process Matrix

The existence of a **unitary extension** of the process matrix, has been proposed as a necessary condition for a process to be physically valid. This concept was initially introduced in [3]<sup>2</sup>, where additional comprehensive information can be found.

Without loss of generality, we can extend the notion of process to encompass a global past  $P$  and a global future  $F$ , which can be seen as additional parties with trivial input (respectively output) space. Mathematically, we can then define a map  $\mathcal{G}_{AB}$  mapping all the input systems of the process to its outputs. In the case of a bipartite process, as given in Figure 3.4, this corresponds to the mapping from  $A'_I, B'_I, P$  to  $A'_O, B'_O, F$ .

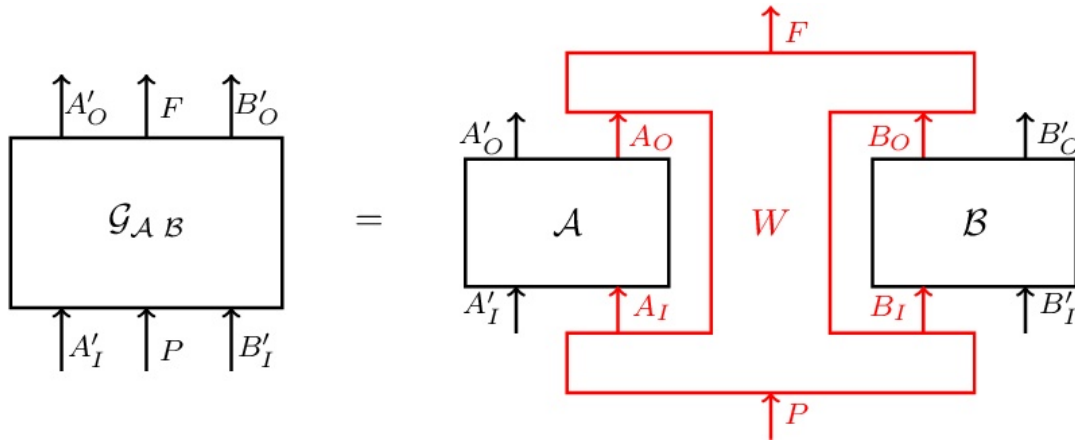


FIGURE 3.4: Illustration of the extension of a bipartite process. As given in Figure 1 of [3].

With such description, a process can equivalently be understood as a map that takes the quantum operations  $\mathcal{A}$  and  $\mathcal{B}$  as inputs and maps them to a global operation  $\mathcal{G}_{AB}$  from the global past  $P$  with the ancillas  $A'_I$  and  $B'_I$  to the global future  $F$  with the ancillas  $A'_O$  and  $B'_O$ .

In [3], two important definitions are introduced:

- A process is a unitary extension if for all unitaries  $\mathcal{A}, \mathcal{B}$ , the resulting  $\mathcal{G}_{AB}$  is a unitary.
- A process is unitarily extendable if one can recover it from a unitary extension by inputting the state  $|0\rangle$  in  $P$  and tracing out  $F$ .

Non unitarily extendable process would correspond to non unitary  $\mathcal{G}_{AB}$  which would not be physical. More details about this notion are given in [3].

<sup>2</sup> Note that in this paper, the unitary extension is referred as purification.

### 3.3 Time-delocalized Subsystems

The concept of **time-delocalized quantum subsystems (TDS)** is a recent development in the context of the process matrix formalism. This notion allows to connect processes with indefinite causal order and temporally ordered quantum circuit from standard QT.

The notion of TDS was initially introduced in [28] with the aim to determine whether causally indefinite processes, in particular the quantum switch, consist in real physical implementation or only a simulation of it. The paper demonstrated that any bipartite processes with indefinite causal order, along with its unitary extension, can be achieved by a temporally ordered quantum circuit, even those with an indefinite causal order. This correspondence can be achieved by changing how quantum circuit operations are described, shifting from acting on subsystems with definite time to subsystems that are not associated with specific times. TDS thus provide a mathematical argument that some processes have a realisation in standard QT. This has been last year generalized to tripartite processes in [34]. We give here an overview presentation of the concept of TDS, for more detailed information on this topic, interested readers can refer to [34]<sup>3</sup>.

In standard QT, the time evolution of a system can be represented using a quantum circuit, where sequences of operations are applied to systems in a well-defined temporal order. Such a circuit can always be divided into fragments which are themselves quantum operations. To illustrate this, Figure 3.5 depicts an arbitrary circuit divided into two fragments: a red fragment and a blue fragment.

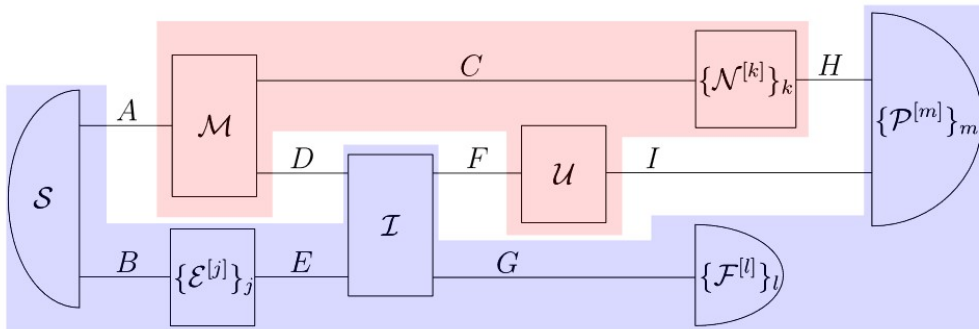


FIGURE 3.5: Illustration of the decomposition of a quantum circuit into two fragments. The circuit consists of various quantum operations. These operations are interconnected through the systems  $A, B, C, D, E, F, G, H, I$ . The red fragment performs a quantum operation on the input systems  $A, F$ , producing output systems  $D, H, I$ , each associated with different time intervals. While the blue fragment, act on  $D, H, I$ , resulting in systems  $A, F$ . As given in Figure 2.a in [34].

In this case, the outgoing systems of the blue fragment are the ingoing systems of the red fragment, and vice versa. and vice versa. The circuit is said to be in a **cyclic** composition.

To describe this, we perform the composition of the fragment using a different choice of systems than in the original circuit. This results in systems that are not associated with a definite time, hence the term "time-delocalized systems".

For example, if we want to compose the red fragment in term of some new system we need to compose it with isomorphism  $J_{in}$  and  $J_{out}$  corresponding to a new tensor product structure on the incoming and outgoing Hilbert spaces. If we also do a composition of

<sup>3</sup> In this paper, the Lugano process is referred as the AF process and its purified form as the BW process.

the blue fragment with the inverse of these isomorphisms, we can compose the fragments back together into a cyclic circuit, as given in Figure 3.6

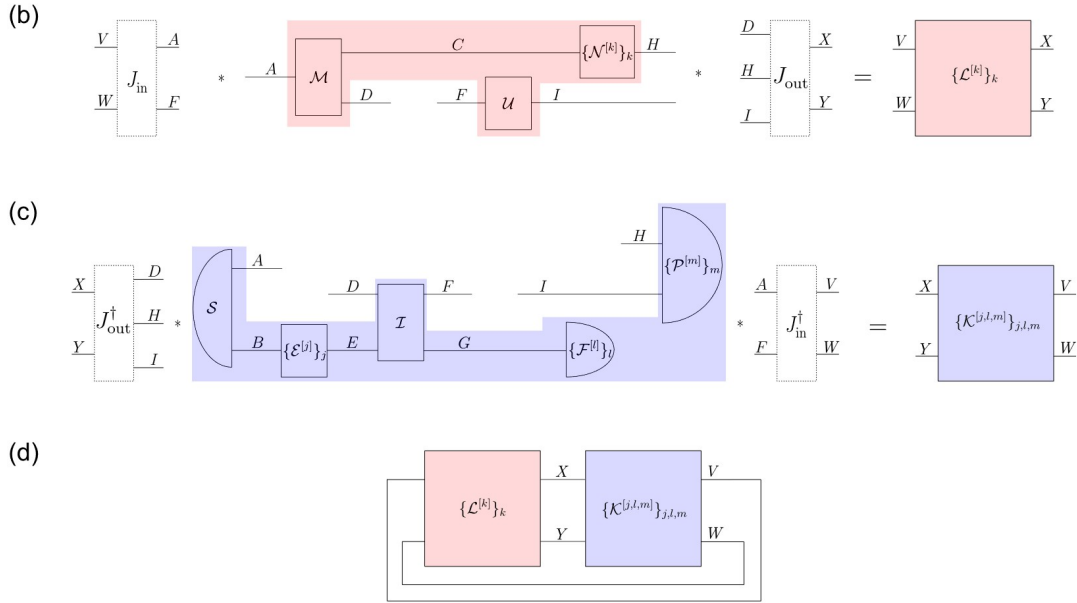


FIGURE 3.6: Illustration of the composition of the two fragments into a cyclic circuit. (b) The red circuit fragment can be described using time-delocalized subsystems  $V, W, X, Y$ , which are defined by the isomorphisms  $J_{in} : H^{VW} \rightarrow H^{AF}$  and  $J_{out} : H^{DHI} \rightarrow H^{XY}$ . This description allow to derive a new operation, denoted  $\{\mathcal{L}^{[k]}\}_k$  from  $V, W$  to  $X, Y$ . (c) Time-delocalized description of the blue fragment in a similar way than for the red fragment. (d) New subsystem description in terms of the time-delocalised subsystems. As given in Figure 2.b,c,d in [34] where more information is provided.

The generalization of TDS to the tripartite case and its application to the Lugano process are of particular interest to us.

### 3.3.1 Generalization to the Tripartite Case

In [34], it was demonstrated that for any unitarily extended tripartite process, the corresponding temporally ordered circuit has a general form as depicted in Figure 3.7.

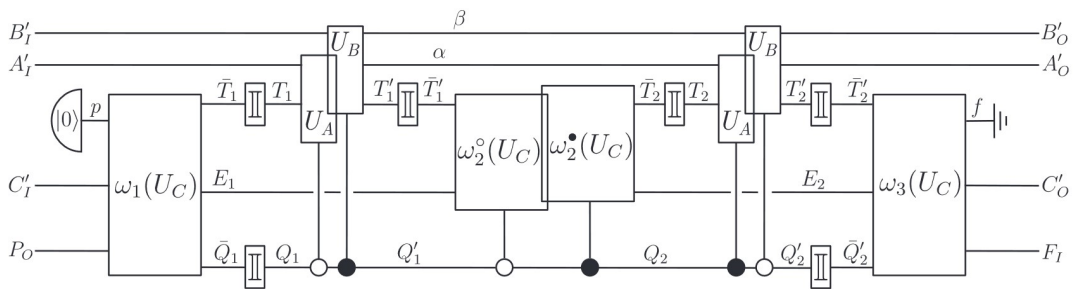


FIGURE 3.7: Temporal circuit for a general tripartite unitary process. As given in Figure 3 of [34] where more information about the circuit is provided.

Where  $A_I, B_I, C_I$  are time-delocalized input systems of the joint system  $T_1 T_2 \bar{T}'_1 \bar{T}'_2 Q_1 P_O$  and  $A_O, B_O, C_O$  are time-delocalized output systems of the joint system  $T'_1 T'_2 \bar{T}_1 \bar{T}_2 Q_2 F_I$ . The operations  $U_A$  and  $U_B$  act on a target system  $T$  depending on the control qubit  $Q$ , and these operations are combined with the circuit operations  $\omega$  which depend on  $U_C$  and

encode information about the process. The computation of the operations  $\omega$  is explained in Section 5 of [35]. Charlie's operation occurs in a time-delocalized manner, neither in the past nor in the future, but on the two possible times. The ancillary system  $P$  is prepared in the state  $|000\rangle$ , and the system  $F$  is discarded.

An important aspect of the quantum switch in the context of TDS is that it was demonstrated in [6, 37] that the set of all unitary extension of unitarily extensible bipartite processes are variations of the quantum switch. Looking at Figure 3.7, one can interpret this circuit as a form of quantum switch where the operation of  $C$  can put the operations of  $A$  and  $B$  in a superposition of causal order.

As previously, the circuit can be decomposed into two fragments, which can then be composed using isomorphisms  $J_{in}$  and  $J_{out}$  to obtain a cyclic circuit, as given in Figure 3.8.

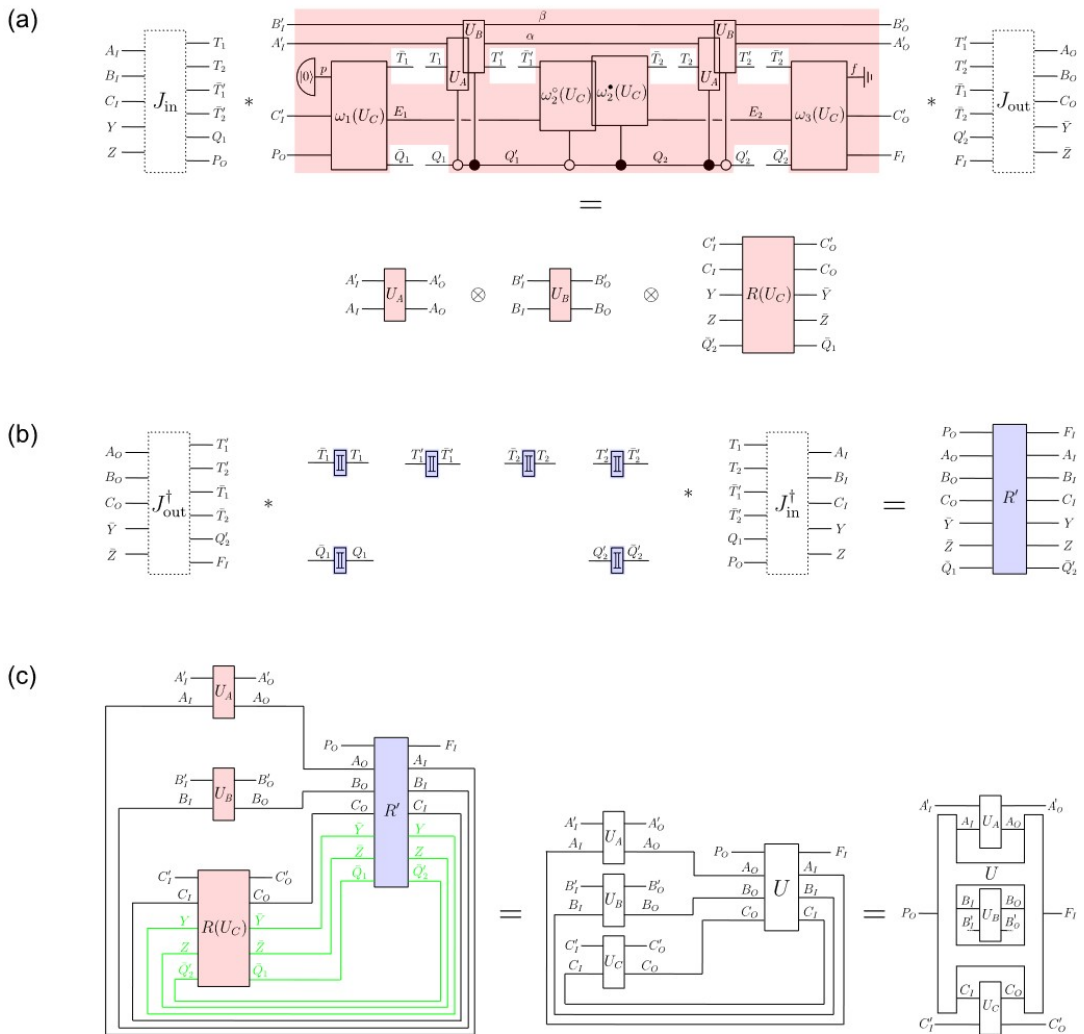


FIGURE 3.8: Description of the tripartite temporal circuit in terms of TDS. (a) Description of the red fragment in terms of time-delocalized subsystems. (b) Description of the blue fragment in terms of time-delocalized subsystems. (c) Composition of the operations  $R(U_C)$  and  $R'$  in a cyclic manner as in the process matrix framework. As given in Figure 4 of [34] where more information is provided.

This description of tripartite processes in terms of TDS is particularly intriguing because the Lugano process, which is known to violate causal inequalities and to possess interesting properties in terms of QNWE, is a unitarily extendible tripartite process. These properties motivated the realization of TDS description of the Lugano process in [34]. This TDS description is shown in Figure 3.9, where we can see that  $U_C$  is applied once with certainty in the beginning and, at some later time, is then reversed and reapplied depending on the action of the other parties. Thus, in any case,  $U_C$  is only applied once in total.

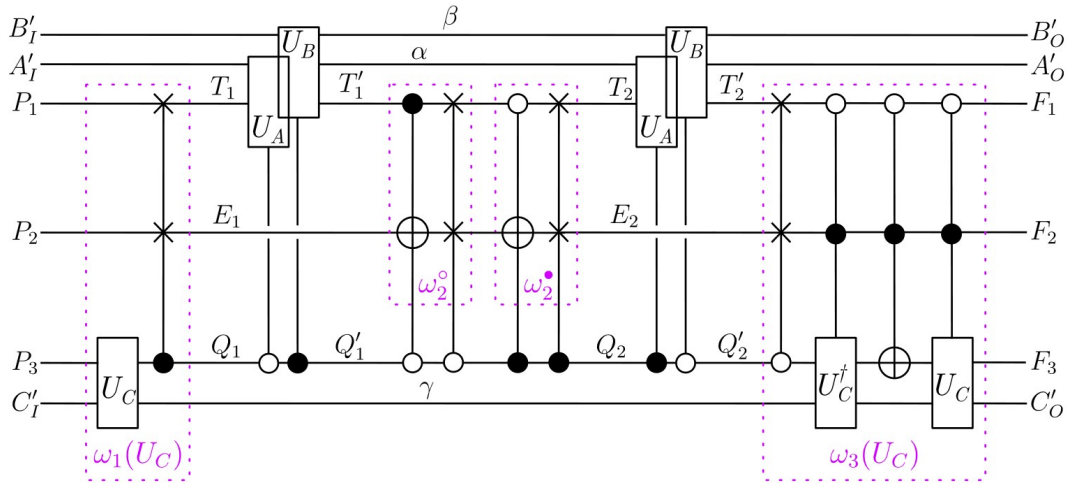


FIGURE 3.9: Description of the Lugano process in terms of TDS. As given in Figure 5 of [34] where more information about the circuit is provided.

## Chapter 4

# Quantum Nonlocality Without Entanglement and Lugano Process

This chapter serves as the final piece of theoretical background necessary to fully understand the results presented in this thesis. We introduce the concepts of **local operation and classical communication (LOCC)**, which are necessary to understand **quantum nonlocality without entanglement (QNWE)**. Additionally, we present a causally indefinite process known as the **Lugano process** and explain how it can be used to achieve something impossible with QNWE in a situation with a well-defined causal order: the establishment of a LOCC protocol that implements the **Shift basis** measurement.

### 4.1 Local Operation and Classical Communication (LOCC)

Considering all possible operations that can be performed on a quantum system, there exists a subset known as **Local Operations and Classical Communication (LOCC)**. This subset involves multiple parties who share certain subsystems of the overall quantum system. The parties are limited to performing actions solely on their respective subsystems, such as carrying out measurements and more general quantum operations. However, they are allowed to communicate the results of their operations through classical means. Typically, the actions performed by the parties depend on the information they receive from each other. [12]

### 4.2 Quantum Nonlocality Without Entanglement

**Quantum Nonlocality Without Entanglement (QNWE)** is a physical property that occurs in a multi-party system when the parties cannot perfectly distinguish quantum states that are separable and orthogonal through local operations and classical communication (LOCC). This phenomenon is remarkable because orthogonal states can be perfectly discriminated in QT. It is only when considering LOCC instead of global measurement that these indistinguishabilities arise.

Demonstrations of QNWE are given in [8, 27].

#### 4.2.1 Shift Basis

The first paper that highlighted QNWE [8] also found a particular set of three-qubit states that cannot be measured locally. This set, which is of interest for this thesis, is a basis of eight unentangled orthogonal states called the **Shift basis**, given by:

$$\{|000\rangle, |111\rangle, | + 01\rangle, | - 01\rangle, |1 + 0\rangle, |1 - 0\rangle, |01+\rangle, |01-\rangle\}$$

where  $|\pm\rangle$  stands for  $\frac{1}{\sqrt{2}}(|0\rangle \pm |1\rangle)$

### 4.3 Lugano Process

Recently, it has been shown [24] that the discrimination of the Shift basis is achievable through the utilization of a specific non-causal process, called the **Lugano process**.<sup>1</sup>

In this tripartite process, each of the three parties are in isolated laboratories, each receiving a bit as input and producing a bit as output. The input and output bits are respectively denoted by  $a, b, c$  and  $x, y, z$ , as shown in Figure 4.1.

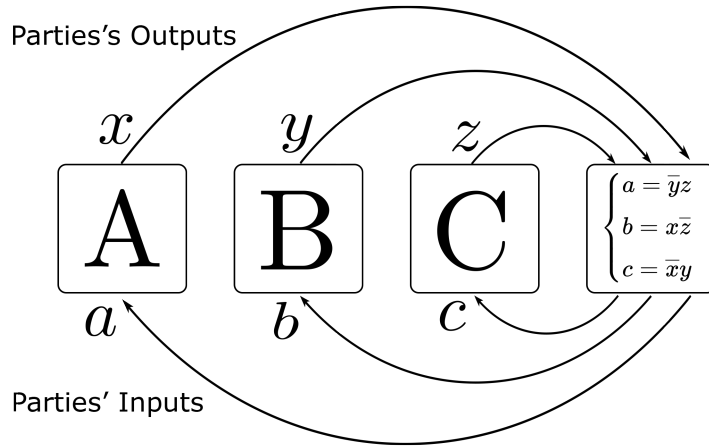


FIGURE 4.1: Representation of the Lugano Process. Each party's input bit is a function of the the output bits of the two other parties.

Each party's input bit is a function of the the output bits of the two other parties according to the following relationships:

$$\begin{cases} a = \bar{y}z \\ b = \bar{x}\bar{z} \\ c = \bar{x}y \end{cases}$$

where  $\bar{x}$  denotes the boolean negation of  $x$ .

Furthermore, it is worth mentioning that the Lugano process is classical within the process matrix framework. In this context, the operations performed by the parties and the process itself are described by classical probability theory. It is important to note that even within this classical setting, causally indefinite processes can be observed when considering more than two parties. Formally, the classical framework serves as a special case of the quantum framework, where all objects are diagonal in the computational basis. Additionally, the Lugano process is deterministic, implying that the corresponding channel is determined entirely by a deterministic function mapping the parties' outputs to their inputs. Circuits corresponding to this process have been studied in [34, 24, 2].

<sup>1</sup> This process was first highlighted in [7] as an extremal point of the deterministic-extrema polytope.



#### 4.4 Lugano process-based LOCC Shift Basis Measurement (LLSBM)

In [24] it was demonstrated a Lugano process-based LOCC Shift basis measurement (LLSBM) can be achieved through the protocol shown in Figure 4.2.

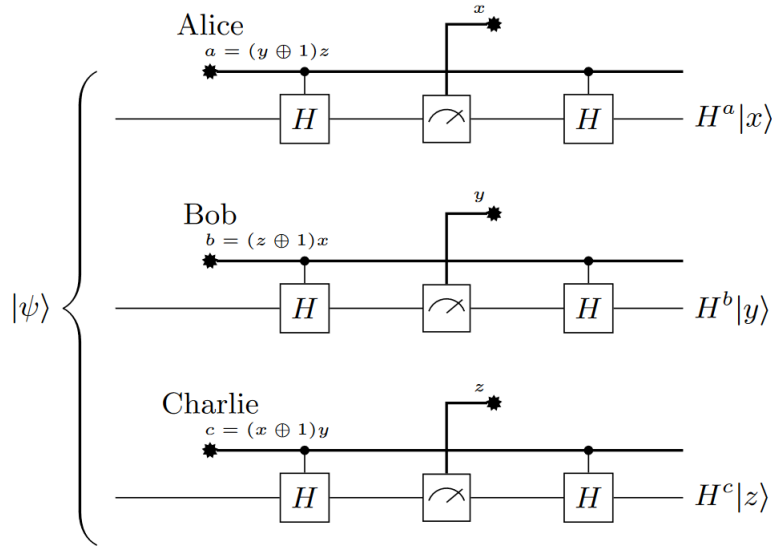


FIGURE 4.2: Schematic of the LOCC implementation of the Shift basis measurement using the Lugano process. Where  $|\psi\rangle$  is an arbitrary input state and  $(*)$  represents the interface to the Lugano process. As featured in [24].

This protocol involves three parties, with identical operations. Let's examine Alice's procedure as an example.

Alice receives a qubit from the unknown input Shift state  $|\psi\rangle$ . Based on the values of  $z$  and  $y$  communicated to her by the Lugano process, she applies a Hadamard gate to her qubit only if  $\bar{y}z = 1$ .<sup>2</sup> After that, she performs a measurement in the computational basis and communicates her result  $x$ . Subsequently, she applies another Hadamard gate to the post-measurement state  $|x\rangle$  with the same condition  $\bar{y}z = 1$ .

It has been proven in [24] that for each input Shift state corresponds a unique measurement result  $(x, y, z)$ , and the protocol successfully retrieves the input state  $|\psi\rangle$  with certainty. This one-to-one correspondence is presented in the Table 4.1.

Shift State	Output State	Shift State	Output State
$ 000\rangle$	$ 000\rangle$	$ 1+0\rangle$	$ 100\rangle$
$ 111\rangle$	$ 111\rangle$	$ 1-0\rangle$	$ 110\rangle$
$ +01\rangle$	$ 001\rangle$	$ 01+\rangle$	$ 010\rangle$
$ -01\rangle$	$ 101\rangle$	$ 01-\rangle$	$ 011\rangle$

TABLE 4.1: Correspondences between the Shift states and the measurement outputs of the protocol of [24].

<sup>2</sup> Note the equivalence  $\bar{y}z = (y \oplus 1)z$ ,  $x\bar{z} = (z \oplus 1)x$  and  $\bar{x}y = (x \oplus 1)y$ .

#### 4.4.1 Quantum Circuit Generating the Shift Basis

In addition to the LLSBM protocol, there is another circuit that successfully replicates the one-to-one correspondence indicated in Table 4.1. This alternative circuit is presented in Figure 4.2, which is featured in [27].

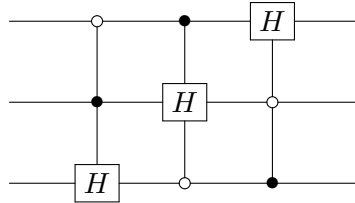


TABLE 4.2: Quantum circuit generating the Shift basis from the computational basis. As established in [27].

However, unlike the previous protocol, this circuit cannot be replaced by a LOCC protocol as it was demonstrated in [27].

## **Part II**

# **Results**

## Chapter 5

# Lugano Process Implementation by the Lugano Circuit

The first result of this thesis is the demonstration that the circuit designed by J. Wechs [33] effectively implements the Lugano process. For readability, we call this circuit the **Lugano circuit**. This circuit was obtained through a private communication with J. Wechs, who established it with the aim of obtaining a simplified version of the time-delocalized description of the Lugano process given in Figure 3.9. This initial step is crucial as we use the Lugano process to reproduce the Shift states measurement from Figure 4.2. We thus need a circuit that implements the Lugano process to conduct our research. A formal proof that the Lugano circuit effectively implements the Lugano process has not yet been carried out, which is why we are doing it here.

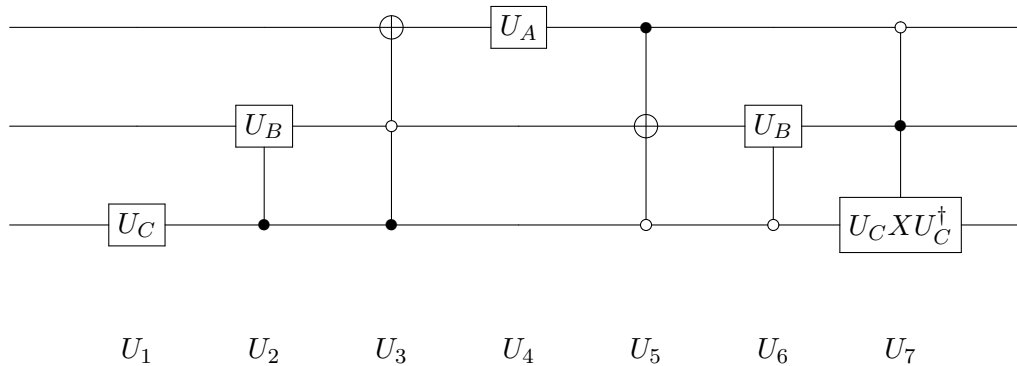


TABLE 5.1: Lugano circuit

In order to prove that the Lugano circuit indeed implements the Lugano process, we demonstrate the equality between two unitary:

- The total unitary that the Lugano circuit implements denoted  $U_{LC}$ .
- The global unitary transformation resulting from the unitary extension of the Lugano process denoted  $U_{LP}$ . It corresponds to  $\mathcal{G}_{AB}$  in Chapter 3.2 but for a tripartite case.

Throughout this demonstration, we will utilize the following notations for the unitaries of the parties:

$$U_A = \begin{bmatrix} a_{00} & a_{01} \\ a_{10} & a_{11} \end{bmatrix} \quad U_B = \begin{bmatrix} b_{00} & b_{01} \\ b_{10} & b_{11} \end{bmatrix} \quad U_C = \begin{bmatrix} c_{00} & c_{01} \\ c_{10} & c_{11} \end{bmatrix}$$

and for the elements of  $U_C X U_C^\dagger$

$$U_C X U_C^\dagger = \begin{bmatrix} c_{01}c_{00}^* + c_{00}c_{01}^* & c_{01}c_{10}^* + c_{00}c_{11}^* \\ c_{11}c_{00}^* + c_{10}c_{01}^* & c_{11}c_{10}^* + c_{10}c_{11}^* \end{bmatrix} = \begin{bmatrix} \lambda_{00} & \lambda_{01} \\ \lambda_{10} & \lambda_{11} \end{bmatrix}$$

## 5.1 Total Unitary of the Lugano Circuit

As indicated in Table 5.1, the Lugano circuit can be decomposed in seven unitaries.

$$U_1 = I \otimes I \otimes U_C$$

$$U_2 = I \otimes (I \otimes |0\rangle\langle 0| + U_B \otimes |1\rangle\langle 1|)$$

$$U_3 = I \otimes |0\rangle\langle 0| \otimes |0\rangle\langle 0| + X \otimes |0\rangle\langle 0| \otimes |1\rangle\langle 1| + I \otimes |1\rangle\langle 1| \otimes |0\rangle\langle 0| + I \otimes |1\rangle\langle 1| \otimes |1\rangle\langle 1|$$

$$U_4 = U_A \otimes I \otimes I$$

$$U_5 = |0\rangle\langle 0| \otimes I \otimes |0\rangle\langle 0| + |0\rangle\langle 0| \otimes I \otimes |1\rangle\langle 1| + |1\rangle\langle 1| \otimes X \otimes |0\rangle\langle 0| + |1\rangle\langle 1| \otimes I \otimes |1\rangle\langle 1|$$

$$U_6 = I \otimes (U_B \otimes |0\rangle\langle 0| + I \otimes |1\rangle\langle 1|)$$

$$U_7 = |0\rangle\langle 0| \otimes |0\rangle\langle 0| \otimes I + |0\rangle\langle 0| \otimes |1\rangle\langle 1| \otimes U_C X U_C^\dagger + |1\rangle\langle 1| \otimes |0\rangle\langle 0| \otimes I + |1\rangle\langle 1| \otimes |1\rangle\langle 1| \otimes I$$

The total unitary  $U_{LC}$  ( $LC$  stands for Lugano circuit) is given by the products of these unitaries.

$$U_{LC} = U_7 U_6 U_5 U_4 U_3 U_2 U_1$$

The matrix representation of this unitary is given in Table 5.2. A numerical code performing this computation is given in Appendix C.

## 5.2 Unitary Transformation resulting from the Unitary Extension of the Lugano Process

The process matrix that corresponds to the Lugano process is given by [3]

$$W = \sum_{abc} |a, b, c\rangle^{ABC_O} \langle a, b, c|^{ABC_O} \otimes |\bar{b}c, a\bar{c}, \bar{a}b\rangle^{ABC_I} \langle \bar{b}c, a\bar{c}, \bar{a}b|^{ABC_I}$$

To compute its unitary extension, we need to make the process reversible. This is done in [3] using the reversible transformation  $|x\rangle \rightarrow |f(x)\rangle$  into  $|x\rangle|y\rangle \rightarrow |x\rangle|y \oplus f(x)\rangle$ . This gives the following expression for the purified process vector.

$$|w\rangle\rangle = \sum_{abc, ijk} |abc\rangle^{ABC_O} |ijk\rangle^P |abc\rangle^F |i \oplus \bar{b}c, j \oplus a\bar{c}, k \oplus \bar{a}b\rangle^{ABC_I}$$

The global unitary  $U_{LP}$  ( $LP$  stands for lugano process), which corresponds to the unitary extension of the Lugano process, can be obtained mathematically by taking the vector link product of the process vector and the pure CJ representation of the parties' operations. Without loss of generality, let's assume that these operations are already unitaries. If this is not the case, the Stinespring dilation theorem allow to dilate the operations to unitaries could always be dilated to unitaries with the addition of ancillary systems. Considering these ancillas would not affect the process this is why we omit them here. The pure CJ representation of the global unitary is given by

$$|U_{LP}\rangle\rangle = |w\rangle\rangle * (|U_A\rangle\rangle \otimes |U_B\rangle\rangle \otimes |U_C\rangle\rangle)$$

$a_{00}b_{00}c_{00}$	$a_{00}b_{00}c_{01}$	$a_{00}b_{01}c_{00}$	$a_{00}b_{01}c_{01}$	$a_{01}b_{00}c_{00}$	$a_{01}b_{00}c_{01}$	$a_{01}b_{01}c_{00}$	$a_{01}b_{01}c_{01}$	$a_{01}b_{01}c_{01}$
$a_{01}b_{00}c_{10}$	$a_{01}b_{00}c_{11}$	$a_{01}b_{01}c_{10}$	$a_{01}b_{01}c_{11}$	$a_{00}b_{00}c_{10}$	$a_{00}b_{00}c_{11}$	$a_{00}b_{01}c_{10}$	$a_{00}b_{01}c_{11}$	$a_{00}b_{01}c_{11}$
$a_{00}b_{10}(c_{00}\lambda_{00} + c_{10}\lambda_{01})$	$a_{00}b_{10}(c_{01}\lambda_{00} + c_{11}\lambda_{01})$	$a_{00}b_{11}(c_{00}\lambda_{00} + c_{10}\lambda_{01})$	$a_{00}b_{11}(c_{01}\lambda_{00} + c_{11}\lambda_{01})$	$a_{01}b_{10}(c_{00}\lambda_{00} + c_{10}\lambda_{01})$	$a_{01}b_{10}(c_{01}\lambda_{00} + c_{11}\lambda_{01})$	$a_{01}b_{11}(c_{00}\lambda_{00} + c_{10}\lambda_{01})$	$a_{01}b_{11}(c_{01}\lambda_{00} + c_{11}\lambda_{01})$	$a_{01}b_{11}(c_{01}\lambda_{00} + c_{11}\lambda_{01})$
$a_{00}b_{10}(c_{00}\lambda_{10} + c_{10}\lambda_{11})$	$a_{00}b_{10}(c_{01}\lambda_{10} + c_{11}\lambda_{11})$	$a_{00}b_{11}(c_{00}\lambda_{10} + c_{10}\lambda_{11})$	$a_{00}b_{11}(c_{01}\lambda_{10} + c_{11}\lambda_{11})$	$a_{01}b_{10}(c_{00}\lambda_{10} + c_{10}\lambda_{11})$	$a_{01}b_{10}(c_{01}\lambda_{10} + c_{11}\lambda_{11})$	$a_{01}b_{11}(c_{00}\lambda_{10} + c_{10}\lambda_{11})$	$a_{01}b_{11}(c_{01}\lambda_{10} + c_{11}\lambda_{11})$	$a_{01}b_{11}(c_{01}\lambda_{10} + c_{11}\lambda_{11})$
$a_{10}b_{01}c_{00}$	$a_{10}b_{01}c_{01}$	$a_{10}b_{00}c_{00}$	$a_{10}b_{00}c_{01}$	$a_{11}b_{01}c_{00}$	$a_{11}b_{01}c_{01}$	$a_{11}b_{01}c_{01}$	$a_{11}b_{00}c_{01}$	$a_{11}b_{00}c_{01}$
$a_{11}b_{00}c_{10}$	$a_{11}b_{00}c_{11}$	$a_{11}b_{01}c_{10}$	$a_{11}b_{01}c_{11}$	$a_{10}b_{00}c_{10}$	$a_{10}b_{00}c_{11}$	$a_{10}b_{01}c_{10}$	$a_{10}b_{01}c_{11}$	$a_{10}b_{01}c_{11}$
$a_{10}b_{11}c_{00}$	$a_{10}b_{11}c_{01}$	$a_{10}b_{10}c_{00}$	$a_{10}b_{10}c_{01}$	$a_{11}b_{11}c_{00}$	$a_{11}b_{11}c_{01}$	$a_{11}b_{11}c_{01}$	$a_{11}b_{10}c_{01}$	$a_{11}b_{10}c_{01}$
$a_{10}b_{10}c_{10}$	$a_{10}b_{10}c_{11}$	$a_{10}b_{11}c_{10}$	$a_{10}b_{11}c_{11}$	$a_{11}b_{10}c_{10}$	$a_{11}b_{10}c_{11}$	$a_{11}b_{11}c_{10}$	$a_{11}b_{11}c_{11}$	$a_{11}b_{11}c_{11}$

TABLE 5.2: Result of the computation of  $U_{LC}$ .

As an example for all parties, we write the pure CJ representation of the unitary of the party  $A$

$$|U_A\rangle\rangle = \sum_{a'} |a'\rangle^{A_I} \otimes U_A |a'\rangle^{A_I}$$

Let's denote by  $H^w$  the Hilbert space of the process vector and  $H^{ABC_{IO}}$  the tensor product of the Hilbert spaces of the incoming and outgoing quantum systems of the parties. The relationships between the Hilbert spaces of the two vectors  $|w\rangle\rangle$  and  $|U_A\rangle\rangle \otimes |U_B\rangle\rangle \otimes |U_C\rangle\rangle$  are

$$\begin{aligned} H^w \cap H^{ABC_{IO}} &= H^{ABC_{IO}} \\ H^w \setminus H^{ABC_{IO}} &= H^{PF} \\ H^{ABC_{IO}} \setminus H^w &= \emptyset \end{aligned}$$

The link product then becomes

$$\begin{aligned} |U_{LP}\rangle\rangle &= \left( I^{PF} \otimes \langle\langle I^{ABC_{IO}ABC_{IO}} \rangle\rangle (|w\rangle\rangle \otimes (|U_A\rangle\rangle \otimes |U_B\rangle\rangle \otimes |U_C\rangle\rangle) \right) \\ &= \sum_{abc, ijk} a_{a, i\oplus\bar{b}c} b_b, j\oplus a\bar{c} c_c, k\oplus\bar{a}b |abc\rangle^F |ijk\rangle^P \end{aligned}$$

where as example for A:  $\langle a|U_A|i\oplus\bar{b}c\rangle = a_{a, i\oplus\bar{b}c}$ .

The unitary  $U_{LP} \in L(H^P, H^F)$  is computed using the inverse CJ isomorphism.

$$U_{LP} = (|U_{LP}\rangle\rangle)^{T_P} = \sum_{abc, ijk} a_{a, i\oplus\bar{b}c} b_b, j\oplus a\bar{c} c_c, k\oplus\bar{a}b |abc\rangle^F \langle ijk|^P$$

The matrix representation of this unitary is given in Table 5.3.

$a_{00}b_{00}c_{00}$	$a_{00}b_{00}c_{01}$	$a_{00}b_{01}c_{00}$	$a_{00}b_{01}c_{01}$	$a_{01}b_{00}c_{00}$	$a_{01}b_{00}c_{01}$	$a_{01}b_{01}c_{00}$	$a_{01}b_{01}c_{01}$
$a_{01}b_{00}c_{10}$	$a_{01}b_{00}c_{11}$	$a_{01}b_{01}c_{10}$	$a_{01}b_{01}c_{11}$	$a_{00}b_{00}c_{10}$	$a_{00}b_{00}c_{11}$	$a_{00}b_{01}c_{10}$	$a_{00}b_{01}c_{11}$
$a_{00}b_{10}c_{01}$	$a_{00}b_{10}c_{00}$	$a_{00}b_{11}c_{01}$	$a_{00}b_{11}c_{00}$	$a_{01}b_{10}c_{01}$	$a_{01}b_{10}c_{00}$	$a_{01}b_{11}c_{01}$	$a_{01}b_{11}c_{00}$
$a_{00}b_{10}c_{11}$	$a_{00}b_{10}c_{10}$	$a_{00}b_{11}c_{11}$	$a_{00}b_{11}c_{10}$	$a_{01}b_{10}c_{11}$	$a_{01}b_{10}c_{10}$	$a_{01}b_{11}c_{11}$	$a_{01}b_{11}c_{10}$
$a_{10}b_{01}c_{00}$	$a_{10}b_{01}c_{01}$	$a_{10}b_{00}c_{00}$	$a_{10}b_{00}c_{01}$	$a_{11}b_{01}c_{00}$	$a_{11}b_{01}c_{01}$	$a_{11}b_{00}c_{00}$	$a_{11}b_{00}c_{01}$
$a_{11}b_{00}c_{10}$	$a_{11}b_{00}c_{11}$	$a_{11}b_{01}c_{10}$	$a_{11}b_{01}c_{11}$	$a_{10}b_{00}c_{10}$	$a_{10}b_{00}c_{11}$	$a_{10}b_{01}c_{10}$	$a_{10}b_{01}c_{11}$
$a_{10}b_{11}c_{00}$	$a_{10}b_{11}c_{01}$	$a_{10}b_{10}c_{00}$	$a_{10}b_{10}c_{01}$	$a_{11}b_{11}c_{00}$	$a_{11}b_{11}c_{01}$	$a_{11}b_{10}c_{00}$	$a_{11}b_{10}c_{01}$
$a_{10}b_{10}c_{10}$	$a_{10}b_{10}c_{11}$	$a_{10}b_{11}c_{10}$	$a_{10}b_{11}c_{11}$	$a_{11}b_{10}c_{10}$	$a_{11}b_{10}c_{11}$	$a_{11}b_{11}c_{10}$	$a_{11}b_{11}c_{11}$

TABLE 5.3: Result of the computation of  $U_{LP}$ .

A comparison between Table 5.2 and Table 5.3 reveals that these two unitaries are nearly identical, with only 16 elements differing between them. To demonstrate the equivalence of these two unitaries, it is necessary to establish the equality of these 16 elements with each other. This is done in the next section.

### 5.3 Equality of Differing Terms

We are looking here to prove the equality between  $U_{LC}$  and  $U_{LP}$ . In order to do this we need to prove the equality between the 16 elements that between the two matrices. Upon examination, several of the 16 equations are identical, leading to the identification of four distinct equations:

$$\begin{aligned} c_{00} &= c_{01}\lambda_{00} + c_{11}\lambda_{01} & c_{01} &= c_{00}\lambda_{00} + c_{10}\lambda_{01} \\ c_{10} &= c_{01}\lambda_{10} + c_{11}\lambda_{11} & c_{11} &= c_{00}\lambda_{10} + c_{10}\lambda_{11} \end{aligned}$$

As  $U_C$  is unitary, we can model it as  $U_C = \begin{bmatrix} a & b \\ -e^{i\phi}b^* & e^{i\phi}a^* \end{bmatrix}$  with  $|a|^2 + |b|^2 = 1$ .

For the first equation,  $c_{00} = c_{01}\lambda_{00} + c_{11}\lambda_{01}$ :

$$a = b(ba^* + ab^*) + e^{i\phi}a^*(-b^2e^{-i\phi} + a^2e^{-i\phi}) = a^*b^2 + a|b|^2 - a^*b^2 + a|a|^2 = a$$

For the second equation,  $c_{01} = c_{00}\lambda_{00} + c_{10}\lambda_{01}$ :

$$b = a(ba^* + ab^*) - e^{i\phi}b^*(-b^2e^{-i\phi} + a^2e^{-i\phi}) = |a|^2b + a^2b^* + |b|^2b - a^2b^* = b$$

To prove the equality for the third and fourth equations, we first need to show that

$$c_{00}c_{01}^* = -c_{10}c_{11}^* \quad \text{and} \quad c_{01}c_{00}^* = -c_{11}c_{10}^*$$

This can be shown as follows:

$$\begin{aligned} c_{00}c_{01}^* + c_{10}c_{11}^* &= ba^* - e^{i\phi}a^*e^{-i\phi}b \\ &= ba^* - a^*b \\ &= 0 \end{aligned}$$

Using this, we now compute the third and fourth equation.

For the third equation,  $c_{10} = c_{01}\lambda_{10} + c_{11}\lambda_{11}$ :

$$\begin{aligned} c_{10} &= c_{01}(c_{11}c_{00}^* + c_{10}c_{01}^*) + c_{11}(c_{11}c_{10}^* + c_{10}c_{11}^*) \\ &= c_{01}(c_{11}c_{00}^* + c_{10}c_{01}^*) + c_{11}(-c_{01}c_{00}^* - c_{00}c_{01}^*) \\ &= c_{01}c_{11}c_{00}^* + c_{01}c_{10}c_{01}^* - c_{11}c_{01}c_{00}^* - c_{11}c_{00}c_{01}^* \\ &= e^{i\phi}a^*a^*b - e^{i\phi}|b|^2b^* - e^{i\phi}a^*a^*b - e^{i\phi}|a|^2b^* \\ &= -e^{i\phi}b^* \end{aligned}$$

For the fourth equation,  $c_{11} = c_{00}\lambda_{10} + c_{10}\lambda_{11}$ :

$$\begin{aligned} c_{11} &= c_{00}(c_{11}c_{00}^* + c_{10}c_{01}^*) + c_{10}(c_{11}c_{10}^* + c_{10}c_{11}^*) \\ &= c_{00}(c_{11}c_{00}^* + c_{10}c_{01}^*) + c_{10}(-c_{01}c_{00}^* - c_{00}c_{01}^*) \\ &= c_{00}c_{11}c_{00}^* + c_{00}c_{10}c_{01}^* - c_{10}c_{01}c_{00}^* - c_{10}c_{00}c_{01}^* \\ &= e^{i\phi}|a|^2a^* - e^{i\phi}ab^*b^* + e^{i\phi}|b|^2a^* + e^{i\phi}ab^*b^* \\ &= e^{i\phi}a^* \end{aligned}$$



We have therefore proved that the two unitaries are equal. The Lugano circuit effectively implements the Lugano process.

In the next chapter, we look at the implementation of the Shift states measurement using the Lugano circuit.

## Chapter 6

# Shift States Distinguishability of the Lugano Circuit

In this chapter, we present an analysis of a circuit that implements the Shift basis measurement. To achieve this circuit, we first devise unitaries that realise the specific operations used in the LLSBM. By incorporating these unitaries into the Lugano circuit, we observe that the resulting circuit exhibits interesting properties that enable a complete Shift basis measurement.

We examine the characteristics of the circuit in terms of QNWE under LOCC. As a result, we develop a LOCC protocol that allows for an almost complete measurement of the Shift basis. Specifically, the protocol is capable of distinguishing between the first six Shift states and detecting the presence of the last two states, although it does not provide a distinction between the two final states.

### 6.1 Design of the Unitaries

We devise here unitaries that can be inserted into the Lugano circuit in order to implement the Shift state measurement based on the LLSBM.

By analyzing the LLSBM, we make 3 observations:

- All three parties perform identical operations, we are thus looking for a single unitary common to all three parties.
- A controlled Hadamard is performed on the Shift state based on the input forwarded by the Lugano process. The Lugano process acts in such a way that the Hadamard operates only when the Shift state is in a superposition state  $|+\rangle$  or  $|-\rangle$ , preventing such states to be measured in the computational basis which would consist in a loss of information over the Shift state. Our unitary needs to keep the same properties and must thus contain an Hadamard acting on the Shift state controlled by the input of the Lugano process.
- A measurement in the computational basis is performed. However, we cannot use this type of measurement since it is not a unitary operation. Instead, we can use a CNOT gate.

Here is the unitary established based on the above discussion:

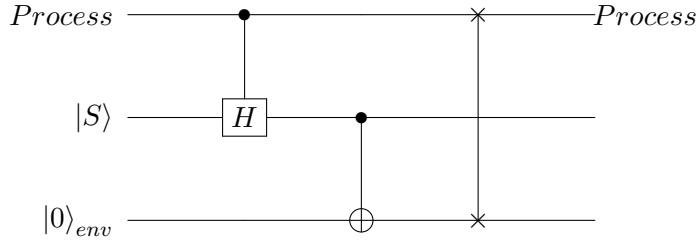


TABLE 6.1: Devised unitary. The first wire of the circuit links the process input to the process output where the Shift state is denoted by  $|S\rangle$  and  $|0\rangle_{env}$  is an environment blank state.

This unitary denoted by  $U$  can be decomposed in the product of 3 unitaries which corresponds to the 3 different gates that compose it.

$$U_1 = (|0\rangle\langle 0| \otimes I + |1\rangle\langle 1| \otimes H) \otimes I$$

$$U_2 = I \otimes (|0\rangle\langle 0| \otimes I + |1\rangle\langle 1| \otimes X)$$

$$U_3 = |0\rangle\langle 0| \otimes I \otimes |0\rangle\langle 0| + |0\rangle\langle 1| \otimes I \otimes |1\rangle\langle 0| + |1\rangle\langle 0| \otimes I \otimes |0\rangle\langle 1| + |1\rangle\langle 1| \otimes I \otimes |1\rangle\langle 1|$$

The implemented unitary is then given by the product of the three.

$$U = U_3 U_2 U_1$$

The development of this product gives as final expression

$$U = |000\rangle\langle 000| + |010\rangle\langle 011| + |001\rangle\langle 1+0| + |011\rangle\langle 1-1| \quad (6.1)$$

$$+ |100\rangle\langle 001| + |110\rangle\langle 010| + |101\rangle\langle 1+1| + |111\rangle\langle 1-0|$$

We have therefore designed a unitary based on the Shift basis measurement protocol using the Lugano process. In next section, we implement this unitary in the Lugano circuit in order to show that it indeed implements the Shift basis measurement.

## 6.2 Implementation of the Unitaries in the Lugano Circuit

Let's insert the devised unitary (Table 6.1) into the gates  $U_A, U_B, U_C, U_C X U_C^\dagger$  from the Lugano circuit (Table 5.1). This results in the following circuit, which is named the **Niedercircuit**.<sup>1</sup> As we will see, the Niedercircuit implements the Shift basis measurement when its input is in the blank state  $|000\rangle^{ABC}$ .

<sup>1</sup> The choice of this name should be perceived as a joking response to the lack of appealing and compact options for the "time-delocalized description of the Lugano circuit implementing the Shift basis measurement". It is important to note that if other researchers were to develop a paper based on these results, we strongly advise them to opt for a more descriptive and serious name. For instance, we would recommend the name "Neithercircuit" because, as we will see later, a LOCC protocol based on the Niedercircuit can't distinguish between neither the  $|01+\rangle$  state nor the  $|01-\rangle$  state.

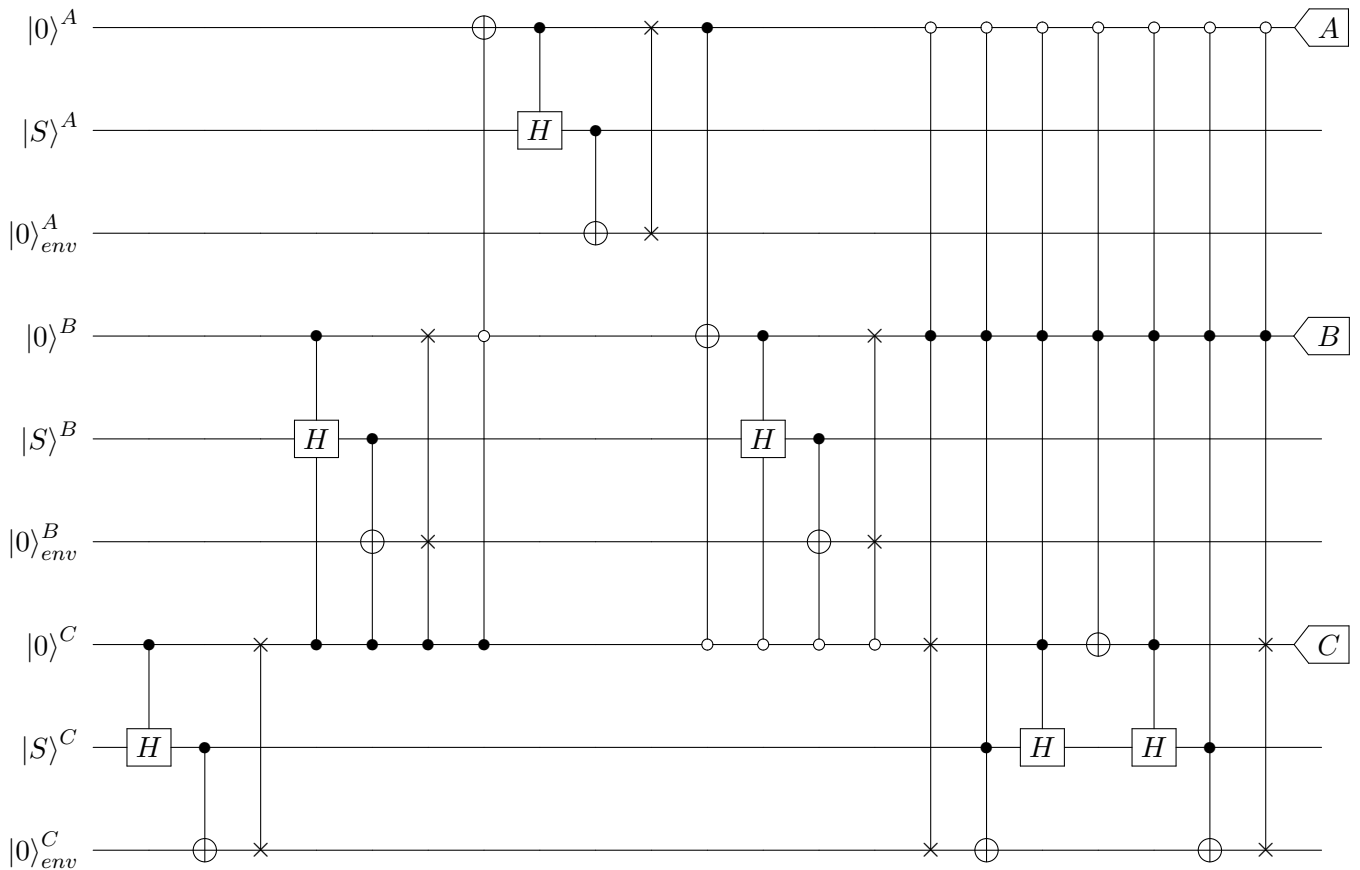


TABLE 6.2: Direct implementation of the devised unitaries into the Lugano circuit. Named the **Niedercircuit**.

Before analysing the properties of the Niedercircuit, there are some simplification that can be done for any input Shift states.

- The first controlled Hadamard is never performed, because its control qubit is always  $|0\rangle^C$ .
- The second controlled Hadamard is never performed, because its control qubit is always  $|0\rangle^B$ .
- The 17th, 18th and 19th unitaries (respectively controlled Hadamard, Toffoli gate and controlled Hadamard) can be merged into one controlled Hadamard that is only performed if the qubits corresponding to the wires  $|0\rangle^A$  and  $|0\rangle^B$  have the correct values. Because if these gates are performed, then the last swap gate of the circuit will also be performed, exchanging the qubit corresponding to the  $|0\rangle^C$  wire with the qubit corresponding to the  $|0\rangle^C_{env}$  wire. As we will see later, we do not care for this last wire, the only outputs of interest of the Niedercircuit is the three wires which are labelled at the end of the circuit by A, B, C.

The simplified version of the Niedercircuit is given below, the analysis that will follow is based on this simplified version but note that it is just as valid as for the above circuit in the context of the Shift basis measurement.

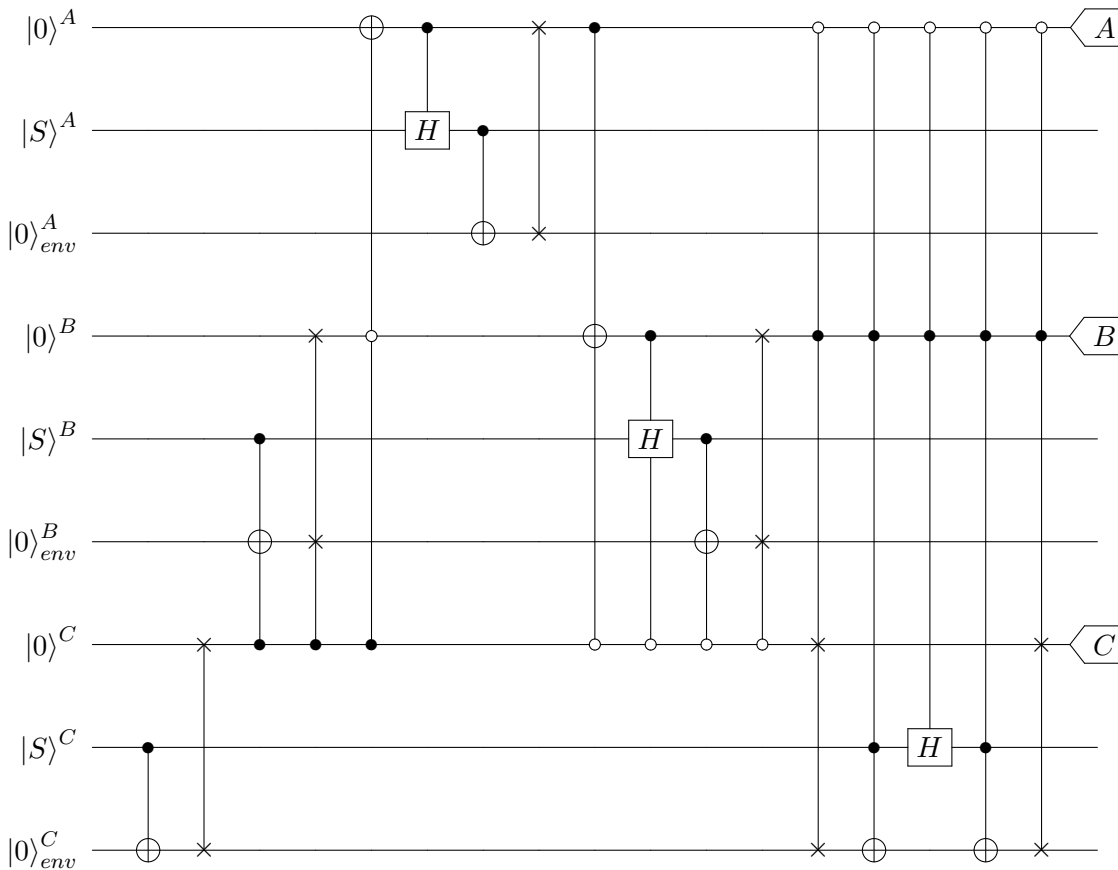


TABLE 6.3: Simplified version of the Nieder circuit

Now that we have the circuit, let's investigate its behaviour for each Shift state.

### 6.3 Shift Basis Measurement of the Nieder circuit

In this section, we examine how the different Shift states evolve through the Nieder circuit. To avoid overwhelming readers with too many details, we will focus on the crucial elements and identify which of the seven unitary operations listed in Table 5.1 are performed for each Shift state. Additionally, we will examine the states at the output of A, B, and C in the Nieder circuit. For those who are interested in a more detailed understanding of the circuit's operation at each step, we recommend to use the quantum circuit simulator provided in [16]. This tool can help visualize the circuit's behavior for any input.

#### 6.3.1 Shift State $|000\rangle$

For this Shift state, all the circuit's input are set to  $|0\rangle$ . In this case, only the non-controlled swap gates are performed, and the input states remain  $|0\rangle$ . The output at A, B, C is therefore  $|000\rangle$ .

#### 6.3.2 Shift State $|111\rangle$

For this Shift state, only the unitaries  $U_1$ ,  $U_2$  and  $U_4$  are performed. This corresponds to performing  $U_A$ ,  $U_B$ , and  $U_C$  once each. Each of the three unitaries generates a  $|1\rangle$  state that remains unchanged until the outputs A, B, C. The output at A, B, C is thus  $|111\rangle$ .

### 6.3.3 Shift State $|+01\rangle$

For this Shift state, only the unitaries  $U_1$ ,  $U_2$ ,  $U_3$  and  $U_4$  are performed. More specifically, the actions of  $U_1$  and  $U_2$  activate  $U_3$  which, in turn, triggers the controlled Hadamard in  $U_4$ . This Hadamard gate sends the Shift state part of A  $|+\rangle^A$  to the state  $|0\rangle^A$ , eliminating the superposition. This behavior, where a controlled Hadamard is activated only to cancel the superposition of a Shift state, repeats for the subsequent Shift states as well. This property of the Niedercircuit is crucial for implementing the complete distinguishability of the Shift basis, as we will discuss further. The output A, B, C is  $|001\rangle$ .

### 6.3.4 Shift State $|−01\rangle$

The Niedercircuit behaves in the same way for this Shift state as for  $|+01\rangle$ , with only the unitaries  $U_1$ ,  $U_2$ ,  $U_3$  and  $U_4$  being performed. The only difference is that the Shift state part of A  $|-\rangle^A$  outputs  $|1\rangle$  instead of  $|0\rangle$  at A. This difference from the output state  $|0\rangle$  to  $|1\rangle$  occurs for every Shift state containing a state in superposition, as the Shift state changes from  $|+\rangle$  to  $|-\rangle$ . The output A, B, C is  $|101\rangle$ .

### 6.3.5 Shift States $|1+0\rangle$ and $|1-0\rangle$

For these two Shift states, only the unitaries  $U_1$ ,  $U_5$  and  $U_6$  are performed. The output A, B, C is  $|100\rangle$  for  $|1+0\rangle$  and  $|110\rangle$  for  $|1-0\rangle$ .

### 6.3.6 Shift States $|01+\rangle$ and $|01-\rangle$

These two last Shift states exhibit more complex behavior compared to the previous ones. This complexity arises because the state  $|S\rangle^C$  is in a superposition which is not cancelled by the Hadamard gate, unlike in the previous Shift states. The output of  $U_1$  is in a superposition that spreads throughout the entire circuit, resulting in a superposition of operations of the unitaries that are both performed and not performed simultaneously.

These two Shift states are the only ones for which all the unitaries are performed, requiring the entire Niedercircuit to distinguish between them. Moreover, these are the only states for which the most complex unitary  $U_7$  is performed, which cancels out any remaining superposition in the circuit.

The output A, B, C is  $|010\rangle$  for  $|01+\rangle$  and  $|011\rangle$  for  $|01-\rangle$ .

### 6.3.7 Summary

Each Shift state given as input to the Niedercircuit corresponds to a unique state of the computational basis, which is determined by the outputs A, B, C. This one-to-one correspondence is presented in the table below.

Shift State	Output State	Shift State	Output State
$ 000\rangle$	$ 000\rangle$	$ 1+0\rangle$	$ 100\rangle$
$ 111\rangle$	$ 111\rangle$	$ 1-0\rangle$	$ 110\rangle$
$ +01\rangle$	$ 001\rangle$	$ 01+\rangle$	$ 010\rangle$
$ −01\rangle$	$ 101\rangle$	$ 01-\rangle$	$ 011\rangle$

TABLE 6.4: Correspondences between the Shift states and the outputs of the Niedercircuit.

It is notable that these correspondences are the same as the ones from the circuits in Figure 4.2 and Table 4.2.

As we have just seen, the Niedercircuit implements quantum operation in its Shift basis measurement. The next sections investigate where this quantumness takes place and the possibility to replace it with LOCC.

## 6.4 LOCC Protocol to Distinguish the Shift Basis

We investigate here how we could use the properties of the Niedercircuit to establish a LOCC protocol to distinguish the Shift basis. We start by presenting a protocol that allows to distinguish between the six first Shift states. We then look at how we could extend this protocol for the two last Shift states and discuss why it's impossible to obtain a complete distinguishability.

### 6.4.1 LOCC Protocol for the six First Shift states

We have devised a LOCC protocol for distinguishing the first six Shift states given by:

$$\{|000\rangle, |111\rangle, | + 01\rangle, | - 01\rangle, |1 + 0\rangle, |1 - 0\rangle, |01+\rangle, |01-\rangle\}$$

This protocol involves Alice, Bob, and Charlie, who communicate with each other classically and each possesses a part of an unknown Shift state. Each in turn, the order of which is determined by what they communicate to each other, must perform on their part of the Shift state the unitary from Table 6.1 where they trigger the Hadamard gate based on the received communication. After completing their unitary, they measure the output state (the state at the end of the top wire of the unitary) in the computational basis and communicate the measurement result to each other. The protocol can be broken down into two steps.

#### First step

Charlie acts first and applies the unitary to his part of the unknown Shift state and performs the measurement in the computational basis. Since Charlie's Shift state is always  $|0\rangle$  or  $|1\rangle$ , his measurement outcome is also always  $|0\rangle$  or  $|1\rangle$ . Charlie then communicates his measurement result to Alice and Bob.

At the end of this step, the parties can already determine a subset of the Shift basis to which the unknown Shift state belongs, as indicated in Table 6.5.

Shift states	$ 000\rangle$	$ 111\rangle$	$  + 01\rangle$	$  - 01\rangle$	$ 1 + 0\rangle$	$ 1 - 0\rangle$
Charlie's result	0	1	1	1	0	0

TABLE 6.5: Result of the first step of the protocol.

The next step depends on Charlie's result.

#### Second step if Charlie communicates 0

If Charlie communicates 0 then the parties know that the Shift state they are trying to distinguish belongs to  $\{|000\rangle, |1 + 0\rangle, |1 - 0\rangle\}$ . In this case, Alice must act second and applies the unitary, measures her output and communicates her outcome. Knowing her

outcome, the subset to which the unknown Shift state belongs shrinks as indicated in Table 6.6.

Shift states	$ 000\rangle$	$ 1+0\rangle$	$ 1-0\rangle$
Alice's result	0	1	1

TABLE 6.6: Result of Alice's measurement.

If the result is 0, the protocol can stop here and the parties know that the Shift state is  $|000\rangle$ .

Otherwise, it remains to distinguish between  $|1+0\rangle$  and  $|1-0\rangle$ . For this, we need Bob to act by performing his unitary but unlike the two previous operations, he must trigger the Hadamard that is in his unitary to prevent the measurement of a superposition state. This result in Table 6.7.

Shift states	$ 1+0\rangle$	$ 1-0\rangle$
Bob's result	0	1

TABLE 6.7: Result of Bob's measurement.

We have thus made a Shift basis measurement in the case where Charlie communicates 0. A symmetric version of this second step happens if Charlie communicates 1.

### Second step if Charlie communicates 1

In this case, the parties are trying to distinguish between  $\{|111\rangle, |+01\rangle, |-01\rangle\}$  In a symmetrical way to the previous case, Bob must act first which result in Table 6.8.

Shift states	$ 111\rangle$	$ +01\rangle$	$ -01\rangle$
Bob's result	1	0	0

TABLE 6.8: Result of Bob's measurement.

It remains to distinguish between  $|+01\rangle$  and  $|-01\rangle$ . For this, Alice acts second and triggers the Hadamard in her unitary which result in Table 6.9.

Shift states	$ +01\rangle$	$ -01\rangle$
Alice's result	0	1

TABLE 6.9: Result of Alice's measurement.

We have therefore a LOCC protocol which allows to distinguish perfectly the first six Shift states. But how does the last two states react to this protocol ? Could we modify the protocol to realize a complete measurement of the Shift basis ? These questions are investigated in next subsection.



### 6.4.2 Protocol on the last two Shift states

First, Charlie applies his unitary. His CNOT thus acts on  $|+0\rangle$  or  $|-0\rangle$ , resulting in a Bell state which is respectively maximally correlated or maximally anticorrelated. Charlie's measurement will collapse the state to either  $|00\rangle$  or  $|11\rangle$ , both with equal probability. Since the same collapse occurs for  $|+\rangle^C$  and  $|-\rangle^C$ , the protocol loses information that could distinguish between them. Therefore, there is a 50-50 chance that Charlie communicates 0 or 1 for both Shift states.

#### Charlie communicates 0

If Charlie communicates 0, then Alice acts second and measures 0 with certainty. At this point, the parties know they are trying to distinguish between the Shift states  $|000\rangle$ ,  $|01+\rangle$ ,  $|01-\rangle$ . Alice then communicates her result of 0 to Bob.

Previously, if Alice communicated 0, the parties could stop the protocol since they knew with certainty that the Shift state was  $|000\rangle$ . However, since the protocol now considers the entire Shift basis, the parties must continue. Bob applies his unitary without triggering the Hadamard gate<sup>2</sup> and measures his qubit. If he measures 0, the parties know the Shift state is  $|000\rangle$ . If he measures 1, the Shift state could be either  $|01+\rangle$  or  $|01-\rangle$ .

#### Charlie communicates 1

And inversely if Charlie communicates 1, then Bob acts and measures 1 with certainty. At this point, the parties know they are trying to distinguish between the subset  $\{|111\rangle, |01+\rangle, |01-\rangle\}$ . Bob then communicates his result of 1 to Alice.

Previously, if Bob communicated 1, the parties could stop the protocol since they knew with certainty that the Shift state was  $|111\rangle$ . However, since the protocol now considers the entire Shift basis, the parties must continue. Alice applies her unitary without triggering the Hadamard gate and measures her qubit. If she measures 1, the parties know the Shift state is  $|111\rangle$ . If she measures 0, the Shift state could be either  $|01+\rangle$  or  $|01-\rangle$ .

#### Summary

To summarise, the measurement result of the protocol when the unknown Shift state is  $|01+\rangle$  or  $|01-\rangle$ , is 0 for Alice, 1 for Bob and either 0 or 1 for Charlie. This measurement result only occurs for these two Shift states. The result of the protocol for each Shift state is given in the table below.

Shift State	Measurement Results	Shift State	Measurement Results
$ 000\rangle$	000	$ 1+0\rangle$	100
$ 111\rangle$	111	$ 1-0\rangle$	110
$ +01\rangle$	001	$ 01+\rangle$	010 or 011
$ -01\rangle$	101	$ 01-\rangle$	010 or 011

TABLE 6.10: Result of the protocol.

The presented protocol provides a way to almost completely distinguish the Shift basis by differentiating the first six Shift states and detecting the presence of the last two Shift states, even though they cannot be perfectly distinguished from each other. This

<sup>2</sup> Bob activates it if Alice communicates 1 and does not activate it if Alice communicates 0

limitation is expected due to QNWE. In practice, this limitation occurs at  $U_1$ , where a measurement of the  $|+\rangle$  or  $|-\rangle$  Shift state leads in a loss of information, rendering the two states indistinguishable. Changing the order of operations among the parties would not resolve the problem, as there will always be two Shift states that, once shared among the parties, are in a superposition state. Regardless of who acts first, there will always be two Shift states for which the first acting party has to collapse a state in superposition, resulting in the indistinguishability between the two states.

Despite not achieving perfect distinguishability, this protocol is still valuable for cases where non-perfect measurements are acceptable.

In the next Chapter, we will investigate the conversion of the Lugano circuit with the implemented unitaries to an acausal circuit described by the process matrix formalism, with the goal to identify where the trade-off between complete distinguishability and indefinite causal order happens.

## Chapter 7

# Description of the Lugano Circuit in the Process Matrix Formalism

The Niedercircuit is designed to reproduce the LLSBM protocol, which enable a complete Shift basis distinguishability at the expense of abandoning definite causal order. Therefore, we believe that by relinquishing the definite causal order for the Niedercircuit, we can create a circuit that allows for perfect distinguishability of the Shift states. By analyzing the behavior of this circuit, we hope to gain insight into the point at which indefinite causal order leads to complete distinguishability.

Instead of working directly with the Niedercircuit, our approach for this conversion is to take back the circuit that implements the general TDS description of the Lugano process, as shown in Figure 3.9. This decision is based on the time-consuming and complex nature of the correspondence calculation, which can be simplified by utilizing the aforementioned circuit. Because certain calculation steps presented in [34] can be leveraged.

Upon examining Figure 3.8, we observe that obtaining the acausal circuit corresponding to the Lugano process requires the composition of four unitaries  $U_A$ ,  $U_B$ ,  $R'$ ,  $R(U_C)$ .

We already possess the expressions for  $U_A$ ,  $U_B$ , and  $U_C$ , as they are the unitaries we designed in Table 6.1. The expression for  $R'$  is provided in equation 30 of the supplementary note in [34]. Since it does not depend on the unitaries we devised, we can utilize this expression as is. The remaining task is to calculate  $R(U_C)$ .

### 7.1 $R(U_C)$ computation

The expression of  $R(U_C)$  for the Lugano process is given in equation 29 of supplementary note of [34]:

$$\begin{aligned}
 & |R(U_C)\rangle\rangle_{C_{IO}C'_{IO}Y\bar{Y}ZZ\bar{Z}\bar{Q}_1\bar{Q}'_2} \\
 &= \left( |U_1^\dagger\rangle\rangle_{C_1ZP_OAB_O} * (|I\rangle\rangle_{A_O\bar{T}'_1} \otimes |I\rangle\rangle_{B_O\bar{T}'_2}) \right) * |\omega_1(U_C)\rangle\rangle_{P_OC'_I\bar{T}'_1E_1\bar{Q}_1} * |\omega_2^\circ(U_C)\rangle\rangle_{\bar{T}'_1E_1\bar{T}'_2E_2} \\
 &\quad * |\omega_3(U_C)\rangle\rangle_{\bar{T}'_2E_2\bar{Q}'_2F_1C'_O} * \left( (|I\rangle\rangle_{\bar{T}'_1A_I} \otimes |I\rangle\rangle_{\bar{T}'_2B_I}) * |U_2^\dagger\rangle\rangle_{AB_1F_1C_O\bar{Z}} \right) \otimes |0\rangle^{\bar{Y}} \otimes |0\rangle^Y \\
 &+ \left( |U_1^\dagger\rangle\rangle_{C_1ZP_OAB_O} * (|I\rangle\rangle_{B_O\bar{T}'_1} \otimes |I\rangle\rangle_{A_O\bar{T}'_2}) \right) * |\omega_1(U_C)\rangle\rangle_{P_OC'_I\bar{T}'_1E_1\bar{Q}_1} * |\omega_2^\bullet(U_C)\rangle\rangle_{\bar{T}'_1E_1\bar{T}'_2E_2} \\
 &\quad * |\omega_3(U_C)\rangle\rangle_{\bar{T}'_2E_2\bar{Q}'_2F_1C'_O} * \left( (|I\rangle\rangle_{\bar{T}'_1B_I} \otimes |I\rangle\rangle_{\bar{T}'_2A_I}) * |U_2^\dagger\rangle\rangle_{AB_1F_1C_O\bar{Z}} \right) \otimes |1\rangle^{\bar{Y}} \otimes |1\rangle^Y
 \end{aligned}$$

The corresponding circuit is

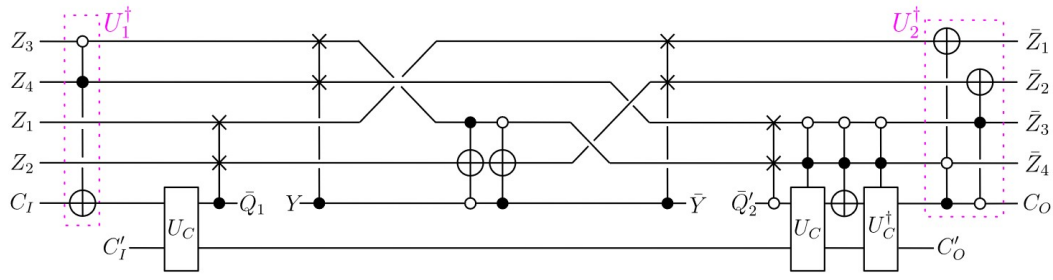


FIGURE 7.1: Circuit representation of  $R(U_C)$  for the Lugano process. As given in supplementary Figure 11 of [34].

Inserting our unitary  $U_C$  given in Table 6.1 gives

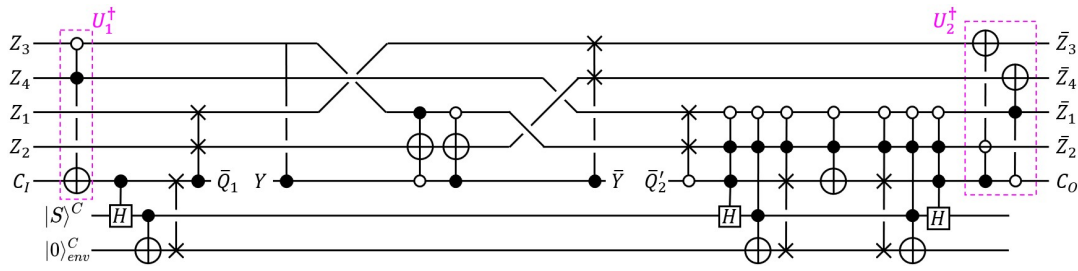


FIGURE 7.2: Circuit representation of  $R(U_C)$  with  $U_C$  given by Table 6.1.

We will first compute each elements of  $R(U_C)$  and then take the composition of all of them.

### 7.1.1 $(|U_1^\dagger\rangle\rangle_{C_I Z P_O A B_O} * (|I\rangle\rangle_{A_O \bar{T}'_1} \otimes |I\rangle\rangle_{B_O \bar{T}'_2})$ computation

$U_1 \in L(H^{P_{123} A B_O}, H^{C_I Z})$  is given in equation 37 of supplementary note of [34]:

$$U_1 = \sum_{\substack{p_1, p_2, p_3 \\ a_o, b_o}} |p_3 \oplus \bar{a}_o b_o\rangle^{C_I} |p_1, p_2, a_o, b_o\rangle^Z \langle p_1, p_2, p_3|^{P_{123}} \langle a_o, b_o|^{A_o B_o}$$

Its conjugate transpose  $U_1^\dagger \in L(H^{C_I Z}, H^{P_{123} A B_O})$  is given by

$$U_1^\dagger = \sum_{\substack{p_1, p_2, p_3 \\ a_o, b_o}} |p_1, p_2, p_3\rangle^{P_{123}} |a_o, b_o\rangle^{A_o B_o} \langle p_3 \oplus \bar{a}_o b_o|^{C_I} \langle p_1, p_2, a_o, b_o|^Z$$

We need to compose the CJ pure representation of  $U_1$  with identity channels that changes the Hilbert spaces on which  $U_1$  acts. This can be computed without using the link product:

$$= \sum_{\substack{p_1, p_2, p_3 \\ a_o, b_o}} |p_1, p_2, p_3\rangle^{P_{123}} |a_o, b_o\rangle^{\bar{T}'_1 \bar{T}'_2} \langle p_3 \oplus \bar{a}_o b_o|^{C_I} \langle p_1, p_2, a_o, b_o|^Z$$

$$\begin{aligned}
|U_1^\dagger\rangle\rangle^{C_I Z P_O A_O B_O} * (|I\rangle\rangle^{A_O \bar{T}'_1} \otimes |I\rangle\rangle^{B_O \bar{T}'_2}) &= \sum_{c, z_{1234}} U_1^\dagger |c, z_{1234}\rangle^{C_I Z} \otimes |c, z_{1234}\rangle^{C_I Z} \\
&= \sum_{\substack{c, z_{1234} \\ p_{123}, a_o, b_o}} |p_1, p_2, p_3\rangle^{P_{123}} |a_o, b_o\rangle^{\bar{T}'_1 \bar{T}'_2} \langle p_3 \oplus \bar{a}_o b_o |^{C_I} \langle p_1, p_2, a_o, b_o |^Z |c, z_1, z_2, z_3, z_4\rangle^{C_I Z} |c, z_1, z_2, z_3, z_4\rangle^{C_I Z} \\
&= \sum_{c, z_{1234}} |z_1, z_2, c \oplus \bar{z}_3 z_4\rangle^{P_{123}} |c, z_{1234}\rangle^{C_I Z}
\end{aligned} \tag{7.1}$$

where we have used  $p_3 \oplus \bar{z}_3 z_4 = c \iff p_3 = \bar{z}_3 z_4 \oplus c$ .

### 7.1.2 $((|I\rangle\rangle^{\bar{T}_1 B_I} \otimes |I\rangle\rangle^{\bar{T}_2 A_I}) * |U_2^\dagger\rangle\rangle^{A B_I F_I C_O \bar{Z}})$ computation

$U_2 \in L(H^{C_O \bar{Z}}, H^{A B_I F_{123}})$  is given in equation 37 of supplementary note of [34]:

$$U_2 = \sum_{\substack{a_o, b_o, c_o \\ p_1, p_2}} |p_1 \oplus \bar{b}_o c_o, p_2 \oplus \bar{c}_o a_o\rangle^{A_I B_I} |a_o, b_o, c_o\rangle^{F_{123}} \langle c_o |^{C_O} \langle p_1, p_2, a_o, b_o |^{\bar{Z}}$$

Using a similar reasoning as for  $U_1$  we obtain

$$\begin{aligned}
& ( (|I\rangle\rangle^{\bar{T}_1 B_I} \otimes |I\rangle\rangle^{\bar{T}_2 A_I}) * |U_2^\dagger\rangle\rangle^{A B_I F_I C_O \bar{Z}} ) \\
&= \sum_{f_{123}, p_{12}} |p_2 \oplus \bar{f}_3 f_1, p_1 \oplus \bar{f}_2 f_3, f_{123}\rangle^{\bar{T}_1 \bar{T}_2 F_{123}} |f_3\rangle^{C_O} |p_1, p_2, f_1, f_2\rangle^{\bar{Z}}
\end{aligned} \tag{7.2}$$

### 7.1.3 $|\omega_1(U_C)\rangle\rangle$ computation

$\omega_1(U_C) \in L(H^{P_{123} C'_I}, H^{\bar{T}_1 E_1 \bar{Q}_1 \gamma})$  is given in equation 33 of supplementary note of [34]:

$$\begin{aligned}
\omega_1(U_C) &= I^{P_1 \rightarrow \bar{T}_1} \otimes I^{P_2 \rightarrow E_1} \otimes \left( (|0\rangle\rangle^{\bar{Q}_1} \langle 0 |^{C_O} \otimes I^{C'_O \rightarrow \gamma} \right) U_C (I^{P_3 \rightarrow C_I} \otimes I^{C'_I}) \\
&\quad + I^{P_1 \rightarrow E_1} \otimes I^{P_2 \rightarrow \bar{T}_1} \otimes \left( (|1\rangle\rangle^{\bar{Q}_1} \langle 1 |^{C_O} \otimes I^{C'_O \rightarrow \gamma} \right) U_C (I^{P_3 \rightarrow C_I} \otimes I^{C'_I})
\end{aligned}$$

where we need to insert our unitary  $U_C$  given in equation 6.1. This insertion gives (by skipping several steps)

$$\omega_1(U_C) = \sum_{p_{123}, c'_{12}} |p_{123}\rangle^{P_{123} C'_I} \otimes \left( (|+\rangle\rangle^{\bar{Q}_1} (|01\rangle^\gamma + |11\rangle^\gamma) + |c'_1 \oplus c'_2\rangle^{\bar{Q}_1} |c'_1 0\rangle^\gamma \right)$$

### 7.1.4 $|\omega_2^\circ(U_C)\rangle\rangle$ and $|\omega_2^\bullet(U_C)\rangle\rangle$ computation

For the Lugano process,  $\omega_2^\circ$  and  $\omega_2^\bullet$  do not depend on  $U_C$ , these are given in equation 34 and 35 of supplementary note of [34]

$$\begin{aligned}
\omega_2^\circ &= |0\rangle^{E_2} \langle 0 |^{\bar{T}'_1} \otimes I^{E_1 \rightarrow \bar{T}_2} + |1\rangle^{E_2} \langle 1 |^{\bar{T}'_1} \otimes \left( |0\rangle^{\bar{T}_2} \langle 1 |^{E_1} + |1\rangle^{\bar{T}_2} \langle 0 |^{E_1} \right) \\
\omega_2^\bullet &= |1\rangle^{E_2} \langle 1 |^{\bar{T}'_1} \otimes I^{E_1 \rightarrow \bar{T}_2} + |0\rangle^{E_2} \langle 0 |^{\bar{T}'_1} \otimes \left( |0\rangle^{\bar{T}_2} \langle 1 |^{E_1} + |1\rangle^{\bar{T}_2} \langle 0 |^{E_1} \right)
\end{aligned}$$

### 7.1.5 $|\omega_3(U_C)\rangle\rangle$ computation

$\omega_3(U_C) \in L(H^{\bar{T}'_2 E \bar{Q}'_2 \gamma}, H^{F_{123} C'_O})$  is given in equation 36 of supplementary note of [34]:

$$\begin{aligned} \omega_3(U_C) = & \left( |000\rangle^{F_{123}} \langle 000|^{\bar{T}'_2 E \bar{Q}'_2} + |001\rangle^{F_{123}} \langle 011|^{\bar{T}'_2 E \bar{Q}'_2} + |100\rangle^{F_{123}} \langle 010|^{\bar{T}'_2 E \bar{Q}'_2} \right. \\ & + |101\rangle^{F_{123}} \langle 101|^{\bar{T}'_2 E \bar{Q}'_2} + |110\rangle^{F_{123}} \langle 110|^{\bar{T}'_2 E \bar{Q}'_2} + |111\rangle^{F_{123}} \langle 111|^{\bar{T}'_2 E \bar{Q}'_2} \left. \right) \\ & + |01\rangle^{F_{12}} \langle 100|^{\bar{T}'_2 E \bar{Q}'_2} \otimes \left( (I^{C_O \rightarrow F_3} \otimes I^{C'_O}) (U_C (|0\rangle^{C_I} \langle 1|^{C_I} + |1\rangle^{C_I} \langle 0|^{C_I}) U_C^\dagger) (|0\rangle^{C_O} \otimes I^{\gamma \rightarrow C'_O}) \right) \\ & + |01\rangle^{F_{12}} \langle 011|^{\bar{T}'_2 E \bar{Q}'_2} \otimes \left( (I^{C_O \rightarrow F_3} \otimes I^{C'_O}) (U_C (|0\rangle^{C_I} \langle 1|^{C_I} + |1\rangle^{C_I} \langle 0|^{C_I}) U_C^\dagger) (|1\rangle^{C_O} \otimes I^{\gamma \rightarrow C'_O}) \right) \end{aligned}$$

After  $U_C$  insertion and going to the pure CJ representation we obtain

$$\begin{aligned} |\omega_3(U_C)\rangle\rangle = & \sum_{t_2, e_2, q_2, \gamma_{12}} |t_2, e_2, q_2, \gamma_{12}\rangle^{\bar{T}'_2 E \bar{Q}'_2 \gamma} \\ & \otimes \left( \left( \langle 000|t_2, e_2, q_2\rangle |000\rangle^{F_{123}} + \langle 001|t_2, e_2, q_2\rangle |001\rangle^{F_{123}} + \langle 010|t_2, e_2, q_2\rangle |100\rangle^{F_{123}} \right. \right. \\ & + \left. \langle 101|t_2, e_2, q_2\rangle |101\rangle^{F_{123}} + \langle 110|t_2, e_2, q_2\rangle |110\rangle^{F_{123}} + \langle 111|t_2, e_2, q_2\rangle |111\rangle^{F_{123}} \right) |\gamma_{12}\rangle^{C'_O} \\ & + \frac{1}{\sqrt{2}} \langle 100|t_2, e_2, q_2\rangle |01\rangle^{F_{12}} \left( |0\rangle^{F_3} |\gamma_1, \bar{\gamma}_2\rangle^{C'_O} + |1\rangle^{F_3} |\bar{\gamma}_1, \bar{\gamma}_2\rangle^{C'_O} \right) \\ & + \frac{1}{\sqrt{2}} \langle 011|t_2, e_2, q_2\rangle |01\rangle^{F_{12}} \left( |0\rangle^{F_3} |\bar{\gamma}_1, \bar{\gamma}_2\rangle^{C'_O} + |1\rangle^{F_3} |\gamma_1, \bar{\gamma}_2\rangle^{C'_O} \right) \end{aligned}$$

Now that we have computed all the vectors, we can compose them.

### 7.1.6 Vectors Composition

We compute here only the first term of the addition in the equation of  $|R(U_C)\rangle\rangle$ , the second term only differs by the term  $|\omega_2\rangle\rangle$  and is thus computed in a similar way. The first term  $|R(U_C)\rangle\rangle$  can be decomposed into four compositions.

#### First composition

Let's set  $|1\rangle = \left( |U_1^\dagger\rangle^{C_I Z P_O A B O} * (|I\rangle^{A O \bar{T}'_1} \otimes |I\rangle^{B O \bar{T}'_2}) \right)$  for which we have already computed the expression in Section 7.1.1. With  $|1\rangle \in H^{C_I Z P_{123} \bar{T}'_1 \bar{T}'_2}$  We compute here  $|2\rangle = |1\rangle * |\omega_1(U_C)\rangle\rangle^{P_O C'_I \bar{T}'_1 E_1 \bar{Q}_1}$ . The relationship between the Hilbert spaces of two vectors  $|1\rangle$  and  $|\omega_1(U_C)\rangle\rangle$  are

$$\begin{aligned} |1\rangle \cap |\omega_1(U_C)\rangle\rangle &= H^{C_I Z \bar{T}'_1 \bar{T}'_2} \\ |1\rangle \setminus |\omega_1(U_C)\rangle\rangle &= H^{P_{123}} \\ |\omega_1(U_C)\rangle\rangle \setminus |1\rangle &= H^{C'_I \bar{T}'_1 E_1 \bar{Q}_1 \gamma} \end{aligned}$$

The resulting vector  $|2\rangle$  is thus in  $H^{C_I C'_I Z \bar{T}'_1 \bar{T}'_2 \bar{T}_1 E_1 \bar{Q}_1 \gamma}$

It is given by

$$|2\rangle = \sum_{c, c'_{12}, z_1, z_3, z_4} |c, c'_{12}, z_1, z_3, z_4\rangle^{C_I C'_I Z \bar{T}'_1 \bar{T}'_2} \left( |00\rangle^\gamma + |10\rangle^\gamma + \sqrt{2}|01\rangle^\gamma + \sqrt{2}|11\rangle^\gamma \right) \\ \left( |0\rangle^{\bar{Q}_1} |z_{12}\rangle^{\bar{T}_1 E_1} + |1\rangle^{\bar{Q}_1} |z_{12}\rangle^{E_1 \bar{T}_1} \right)$$

### Third composition

We compute here  $|3\rangle = |2\rangle * |\omega_2^o\rangle\rangle^{\bar{T}'_1 E_1 \bar{T}_2 E_2}$ . The relationship between the Hilbert spaces of two vectors  $|2\rangle$  and  $|\omega_2^o\rangle\rangle$  are

$$|2\rangle \cap |\omega_2^o\rangle\rangle = H^{C_I C'_I Z \bar{T}'_2 \bar{T}_1 \bar{Q}_1 \gamma}$$

$$|2\rangle \setminus |\omega_2^o\rangle\rangle = H^{\bar{T}'_1 E_1}$$

$$|\omega_2^o\rangle\rangle \setminus |2\rangle = H^{\bar{T}_2 E_2}$$

The resulting vector  $|3\rangle$  is thus in  $H^{\in C_I C'_I Z \bar{T}'_2 \bar{T}_1 \bar{Q}_1 \gamma \bar{T}_2 E_2}$

It is given by

$$|3\rangle = \sum_{c, c'_{12}, z_1, z_3, z_4} |c, c'_{12}, z_1, z_3, z_4\rangle^{C_I C'_I Z \bar{T}'_2 \bar{T}_2} \left( |00\rangle^\gamma + |10\rangle^\gamma + \sqrt{2}|01\rangle^\gamma + \sqrt{2}|11\rangle^\gamma \right) \\ \left( |0\rangle^{\bar{Q}_1} |z_1, z_3 \oplus z_2\rangle^{\bar{T}_1 \bar{T}_2} + |1\rangle^{\bar{Q}_1} |z_2, z_3 \oplus z_1\rangle^{\bar{T}_1 \bar{T}_2} \right)$$

### Fourth composition

We compute here  $|4\rangle = |3\rangle * |\omega_3(U_c)\rangle\rangle^{\bar{T}'_2 E_2 \bar{Q}'_2 \gamma F_{123} C'_O}$ . The relationship between the Hilbert spaces of the two vectors  $|3\rangle$  and  $|\omega_3(U_c)\rangle\rangle$  are

$$|3\rangle \cap |\omega_3(U_c)\rangle\rangle = H^{C_I C'_I Z \bar{T}'_1 \bar{Q}_1 \bar{T}_2}$$

$$|3\rangle \setminus |\omega_3(U_c)\rangle\rangle = H^{E_2 \bar{T}'_2 \gamma}$$

$$|\omega_3(U_c)\rangle\rangle \setminus |3\rangle = H^{\bar{Q}'_2 F_{123} C'_O}$$

The resulting vector  $|4\rangle$  is thus in  $H^{C_I C'_I Z \bar{T}'_1 \bar{Q}_1 \bar{T}_2 \bar{Q}'_2 F_{123} C'_O}$

It is given by

$$\begin{aligned}
|4\rangle &= \sum_{\substack{c, c'_{12}, z_{1234}, q_2 \\ q_2, \gamma_{12}}} |c, c'_{12}, z_{1234}, q_2\rangle^{C_I C'_I Z \bar{Q}'_2} (\sqrt{2}\gamma_2 + \bar{\gamma}_2) \\
&\otimes \left( |0\rangle^{\bar{Q}_1} |z_1, z_3 \oplus z_2\rangle^{\bar{T}_1 \bar{T}_2} + |1\rangle^{\bar{Q}_1} |z_2, z_3 \oplus z_1\rangle^{\bar{T}_1 \bar{T}_2} \right) \\
&\otimes \left( \left( \langle 000 | z_4, z_3, q_2 \rangle |000\rangle^{F_{123}} + \langle 001 | z_4, z_3, q_2 \rangle |001\rangle^{F_{123}} + \langle 010 | z_4, z_3, q_2 \rangle |100\rangle^{F_{123}} \right. \right. \\
&+ \langle 101 | z_4, z_3, q_2 \rangle |101\rangle^{F_{123}} + \langle 110 | z_4, z_3, q_2 \rangle |110\rangle^{F_{123}} + \left. \langle 111 | z_4, z_3, q_2 \rangle |111\rangle^{F_{123}} \right) |\gamma_{12}\rangle^{C'_O} \\
&+ \frac{1}{\sqrt{2}} \langle 100 | z_4, z_3, q_2 \rangle |01\rangle^{F_{12}} \left( |0\rangle^{F_3} |\gamma_1, \bar{\gamma}_2\rangle^{C'_O} + |1\rangle^{F_3} |\bar{\gamma}_1, \bar{\gamma}_2\rangle^{C'_O} \right) \\
&+ \frac{1}{\sqrt{2}} \langle 011 | z_4, z_3, q_2 \rangle |01\rangle^{F_{12}} \left( |0\rangle^{F_3} |\bar{\gamma}_1, \bar{\gamma}_2\rangle^{C'_O} + |1\rangle^{F_3} |\gamma_1, \bar{\gamma}_2\rangle^{C'_O} \right)
\end{aligned}$$

### Fifth composition

Let's set  $|5\rangle = \left( (|I\rangle)^{\bar{T}_1 A_I} \otimes (|I\rangle)^{\bar{T}_2 B_I} * |U_2^\dagger\rangle^{AB_I F_{123} C_O \bar{Z}} \right) \otimes |0\rangle^{\bar{Y}} \otimes |0\rangle^{\bar{Y}}$  for which we have already computed the expression in Section 7.1.2. We compute here the final expression of the first term of the addition in  $R(U_C)$  which is equal to  $|4\rangle * |5\rangle$

The relationship between the Hilbert spaces of the two vectors  $|4\rangle$  and  $|5\rangle$  are

$$\begin{aligned}
|4\rangle \cap |5\rangle &= H^{C_I C'_I Z \bar{Q}_1 \bar{Q}'_2 C'_O} \\
|4\rangle \setminus |5\rangle &= H^{\bar{T}_1 \bar{T}_2 F_{123}} \\
|5\rangle \setminus |4\rangle &= H^{C_O \bar{Z}}
\end{aligned}$$

The resulting vector  $|5\rangle$  is thus in  $H^{C_I C'_I C_O C'_O \bar{Q}_1 \bar{Q}'_2 Z \bar{Z}}$  and is given as the first term of the addition in next section.

### 7.1.7 Final Result

The final computed value of  $|R(U_C)\rangle$  is given below as an addition of two terms where the first term was calculated in previous section and the second was obtained with a



similar computation.  $|R(U_C)\rangle\rangle^{CC'_{IO}Y\bar{Y}Z\bar{Z}\bar{Q}_1\bar{Q}'_2} =$

$$\begin{aligned}
& \sum_{\substack{c, c'_{12}, z_{1234}, q_2 \\ \gamma_{12}, p_{12}, f_{123}}} |c, c'_{12}, z_{1234}, q_2\rangle^{CC'_{IO}Z\bar{Q}'_2} |f_3\rangle^{C_o} |p_{12}, f_{12}\rangle^{\bar{Z}} |00\rangle^{Y\bar{Y}} (\gamma_2\sqrt{2} + \bar{\gamma}_2) \\
& \left( \langle p_1 \oplus \bar{f}_2 f_3 | z_1 \rangle \langle p_2 \oplus \bar{f}_3 f_1 | z_3 \oplus z_2 \rangle |0\rangle^{\bar{Q}_1} + \langle p_1 \oplus \bar{f}_2 f_3 | z_2 \rangle \langle p_2 \oplus \bar{f}_3 f_1 | z_3 \oplus z_1 \rangle |1\rangle^{\bar{Q}_1} \right) \\
& \left( \left( \langle 000 | z_4 z_3 q_2 \rangle \langle f_{123} | 000 \rangle + \langle 001 | z_4 z_3 q_2 \rangle \langle f_{123} | 001 \rangle + \langle 010 | z_4 z_3 q_2 \rangle \langle f_{123} | 100 \rangle \right. \right. \\
& \left. \left. + \langle 101 | z_4 z_3 q_2 \rangle \langle f_{123} | 101 \rangle + \langle 110 | z_4 z_3 q_2 \rangle \langle f_{123} | 110 \rangle + \langle 111 | z_4 z_3 q_2 \rangle \langle f_{123} | 111 \rangle \right) |\gamma_{12}\rangle^{C'_o} \right. \\
& \left. + \frac{1}{\sqrt{2}} \langle 100 | z_4 z_3 q_2 \rangle \langle f_{12} | 01 \rangle \left( \langle f_3 | 0 \rangle |\gamma_1, \bar{\gamma}_2\rangle^{C'_o} + \langle f_3 | 1 \rangle |\bar{\gamma}_1, \bar{\gamma}_2\rangle^{C'_o} \right) \right. \\
& \left. + \frac{1}{\sqrt{2}} \langle 011 | z_4 z_3 q_2 \rangle \langle f_{12} | 01 \rangle \left( \langle f_3 | 0 \rangle |\bar{\gamma}_1, \bar{\gamma}_2\rangle^{C'_o} + \langle f_3 | 1 \rangle |\gamma_1, \bar{\gamma}_2\rangle^{C'_o} \right) \right) \\
& + \sum_{\substack{c, c'_{12}, z_{1234}, q_2 \\ \gamma_{12}, p_{12}, f_{123}}} |c, c'_{12}, z_{1234}, q_2\rangle^{CC'_{IO}Z\bar{Q}'_2} |f_3\rangle^{C_o} |p_{12}, f_{12}\rangle^{\bar{Z}} |11\rangle^{Y\bar{Y}} (\gamma_2\sqrt{2} + \bar{\gamma}_2) \\
& \left( \langle p_2 \oplus \bar{f}_3 f_1 | z_1 \rangle \langle p_1 \oplus \bar{f}_2 f_3 | z_4 \oplus z_2 \rangle |0\rangle^{\bar{Q}_1} + \langle p_2 \oplus \bar{f}_3 f_1 | z_2 \rangle \langle p_1 \oplus \bar{f}_2 f_3 | z_4 \oplus z_1 \rangle |1\rangle^{\bar{Q}_1} \right) \\
& \left( \left( \langle 000 | z_4 z_3 q_2 \rangle \langle f_{123} | 000 \rangle + \langle 001 | z_4 z_3 q_2 \rangle \langle f_{123} | 001 \rangle + \langle 010 | z_4 z_3 q_2 \rangle \langle f_{123} | 100 \rangle \right. \right. \\
& \left. \left. + \langle 101 | z_4 z_3 q_2 \rangle \langle f_{123} | 101 \rangle + \langle 110 | z_4 z_3 q_2 \rangle \langle f_{123} | 110 \rangle + \langle 111 | z_4 z_3 q_2 \rangle \langle f_{123} | 111 \rangle \right) |\gamma_{12}\rangle^{C'_o} \right. \\
& \left. + \frac{1}{\sqrt{2}} \langle 100 | z_4 z_3 q_2 \rangle \langle f_{12} | 01 \rangle \left( \langle f_3 | 0 \rangle |\gamma_1, \bar{\gamma}_2\rangle^{C'_o} + \langle f_3 | 1 \rangle |\bar{\gamma}_1, \bar{\gamma}_2\rangle^{C'_o} \right) \right. \\
& \left. + \frac{1}{\sqrt{2}} \langle 011 | z_4 z_3 q_2 \rangle \langle f_{12} | 01 \rangle \left( \langle f_3 | 0 \rangle |\bar{\gamma}_1, \bar{\gamma}_2\rangle^{C'_o} + \langle f_3 | 1 \rangle |\gamma_1, \bar{\gamma}_2\rangle^{C'_o} \right) \right)
\end{aligned}$$

This final result appears to be of significant size and complexity, making its interpretation challenging. The result is not diagonal in the computational basis, showing that it is not a classical transformation.

We believe that composing this result with the unitary transformation labeled as  $R'$  in Figure 3.8 would yield a classical process. If this is indeed the case, we expect that the composition of the four unitaries,  $U_A$ ,  $U_B$ ,  $R'$ , and  $R(U_C)$ , would result in a unitary transformation that is diagonal in the computational basis and that would enable the accomplishment of the complete LOCC Shift basis measurement.

To gain further insights, it would be necessary to conduct investigations into this composition. The conclusion in next chapter provides more detailed explanations regarding these additional investigations.

## Chapter 8

# Conclusion and Further Investigations

The aim of this master's thesis is to investigate the behavior of the implementation of the Shift basis measurement protocol exploiting the Lugano process into a temporally ordered circuit implementing this process. This was done in previous chapters by first demonstrating the equivalence of the Lugano circuit with the Lugano process. Subsequently, a unitary inspired by the Shift basis measurement protocol was designed and inserted into the Lugano circuit, resulting in the Niedercircuit. It was shown that this Niedercircuit allows for complete distinction of the Shift states, and its operation enabled to design a LOCC protocol that allows to distinguish the six first Shift states and to know if we are in the presence of the last two without being able to distinguish them. Following this, an attempt was made to identify the trade-off between complete distinguishability under LOCC and indefinite causal order. This was achieved by computing the unitary  $R(U_C)$ , which exhibits significant complexity and is not diagonal in the computational basis.

The next logical steps in order to understand where the trade between QNWE and causal order would be to compose the four unitaries,  $U_A$ ,  $U_B$ ,  $R'$ , and  $R(U_C)$  to obtain an acausal circuit. Analyzing this circuit, particularly in terms of the capabilities that the individual unitaries cannot achieve separately, may provide the key to understanding this phenomenon.

A research question that formulates these further explorations is "*Does the composition of the four unitaries result in a classical behavior? If so, what causes this transition to classicality? What is the fundamental step that corresponds to the trade-off between indefinite causal order and QNWE?*".

The exploration of these questions is left for future research endeavors.

## Appendix A

# Appendices to Chapter 1

## A.1 Spacetime Interval between two Events

In this appendix, we give some insights into the concepts of causal relationships between events in spacetime by defining the notion of **spacetime interval** between two events and interpreting it.

Let's consider two events that occur at  $(x_1, y_1, z_1, t_1)$  and  $(x_2, y_2, z_2, t_2)$ . We define the spacetime interval between these two events:

$$\Delta\sigma^2 := -(c\Delta t)^2 + \Delta x^2 + \Delta y^2 + \Delta z^2$$

Using Pythagoras' theorem, one can see that  $\Delta x^2 + \Delta y^2 + \Delta z^2$  corresponds to the spatial distance separating the two events squared, let's denote it by  $d^2$ .

$$\iff \Delta\sigma^2 := -c^2\Delta t^2 + d^2$$

Where  $c\Delta t$  is the distance that light travels in that interval of time.

The space time interval thus compares, for the two events, the spatial distance with the light speed distance.

As nothing (no object, no information) can travel faster than light, any event's influence can only affect another if it can be transmitted between them without exceeding the speed of light. The **light cone** is defined as the boundary within which an event can cause another. In other words, causal influence between events is contained within their light cones.

From this last consideration, the space time interval can be used to cast light on the causality relations between the events:

- If  $\Delta\sigma^2 < 0$ , then  $d^2 < c^2\Delta t^2$  : The spatial distance is less than the light speed distance, the interval is called *time-like*. In this case, there exists a reference frame in which both events occur in the same place (for example by being in translation in a direction going from one event to the other at a speed  $v = \frac{d}{\Delta t} < c$ ). The information of the realization of an event can reach the other, they are each in the light cone of the other, thus a causal relation can exist between the two.
- If  $\Delta\sigma^2 = 0$ , then  $d^2 = c^2\Delta t^2$  : The spatial distance is equal to the light speed distance, the interval is called *light-like*. This is an intermediate case where the two

events are each on the surface of the light cone of the other, a causal relation can exist between the two only if the information propagates at a speed  $c$ .

- If  $\Delta\sigma^2 > 0$ , then  $d^2 > c^2\Delta t^2$ : The spatial distance is greater than the light speed distance, the interval is called *space-like*. In this case, the events are spatially too far apart to have caused or influenced the other. They are each outside of the light cone of the other.

Let's note that the spacetime interval is an invariant for any inertial reference frame, in the same way that  $\Delta s^2 = \Delta x^2 + \Delta y^2 + \Delta z^2$  is invariant in Newtonian mechanics.

In general relativity, as gravity deflects and delays light signals, the events' light cones are deformed, that's why the causal structure is said to be dynamic.

## Appendix B

# Appendices to Chapter 2

### B.1 Linear Operator

A **linear operator**  $A$  is a mapping between two vector spaces<sup>1</sup>  $A : H^X \rightarrow H^Y$  (denoted by  $A \in L(H^X, H^Y)$ ) that preserves the operations of vector addition and scalar multiplication

$$A : |\psi\rangle = \sum_i \psi_i |i\rangle \longrightarrow A(|\psi\rangle) = A\left(\sum_i \psi_i |i\rangle\right) = \sum_i \psi_i A(|i\rangle)$$

Where  $A(|\psi\rangle)$  is commonly denoted by  $A|\psi\rangle$ .

A linear operator can be described using its matrix representation. This corresponds to considering the linear operator as a  $m = d_X$  by  $n = d_Y$  matrix mapping vectors from  $H^X$  to  $H^Y$  through matrix multiplication. This matrix representation depends on the choice of basis. Let  $|x_i\rangle$  and  $|y_j\rangle$  be two bases of  $H^X$  and  $H^Y$  respectively, then the matrix elements of the operator are given by  $\langle y_j | A | x_i \rangle$ .

$$A = \begin{bmatrix} \langle y_1 | A | x_1 \rangle & \langle y_1 | A | x_2 \rangle & \dots & \langle y_1 | A | x_n \rangle \\ \langle y_2 | A | x_1 \rangle & \ddots & & \vdots \\ \vdots & & \ddots & \vdots \\ \langle y_m | A | x_1 \rangle & \dots & \dots & \langle y_m | A | x_n \rangle \end{bmatrix}_{m \times n}$$

Such that if  $A|\psi\rangle = |\phi\rangle$  with  $|\psi\rangle = \sum_i \psi_i |x_i\rangle \in H^X$  and  $|\phi\rangle = \sum_i \phi_i |y_i\rangle \in H^Y$  then

$$\begin{bmatrix} \langle y_1 | A | x_1 \rangle & \langle y_1 | A | x_2 \rangle & \dots & \langle y_1 | A | x_n \rangle \\ \langle y_2 | A | x_1 \rangle & \ddots & & \vdots \\ \vdots & & \ddots & \vdots \\ \langle y_m | A | x_1 \rangle & \dots & \dots & \langle y_m | A | x_n \rangle \end{bmatrix}_{m \times n} \begin{bmatrix} \psi_1 \\ \psi_2 \\ \vdots \\ \psi_n \end{bmatrix}_{n \times 1} = \begin{bmatrix} \phi_1 \\ \phi_2 \\ \vdots \\ \phi_m \end{bmatrix}_{m \times 1}$$

A linear operator  $A$  is said to be defined on a vector space  $H^X$  when  $A : H^X \rightarrow H^X$ .

<sup>1</sup> Hilbert spaces in the context of this thesis.

## B.2 Trace

The **trace** of an operator  $A$  is defined as the sum of the diagonal elements of  $A$  with respect to an arbitrary orthonormal basis  $\{|i\rangle\}$ .

$$\text{tr}(A) = \sum_i \langle i|A|i\rangle$$

A significant property of the trace is that it is invariant under a change of basis.

### B.2.1 Partial trace

Given a linear operator  $A \in L(H^{XY})$ , the **partial trace** of  $A$  over  $H^X$  is a way of extracting information about the behavior of  $A$  on  $H^Y$  alone. It is given by

$$\text{tr}_X(A) = \sum_i \langle i_X|A|i_X\rangle$$

Or more explicitly by

$$\text{tr}_X(A) = \sum_i (\langle i_X| \otimes I_Y) A (|i_X\rangle \otimes I_Y)$$

## Appendix C

# Appendices to Chapter 5

## C.1 Numerical Computation of the Total Unitary of the Lugano Circuit

The following Python code allows to compute the total unitary that the Lugano circuit implements. The package SympPy used here allows to manipulate tensor products of matrices with symbolic variables.

```

1  import sympy as sp
2  import sympy.physics.quantum as spq
3
4  # Initialisation of the different variables
5  a00, a01, phi_a = sp.symbols('a00 a01 phi_a')
6  b00, b01, phi_b = sp.symbols('b00 b01 phi_b')
7  c00, c01, phi_c = sp.symbols('c00 c01 phi_c')
8
9  # Representation of the 3 unitaries in the computational basis
10 a10 = - sp.exp(sp.I * phi_a) * sp.conjugate(a01)
11 a11 = sp.exp(sp.I * phi_a) * sp.conjugate(a00)
12 Ua = sp.Matrix([[a00, a01], [a10, a11]])
13
14 b10 = - sp.exp(sp.I * phi_b) * sp.conjugate(b01)
15 b11 = sp.exp(sp.I * phi_b) * sp.conjugate(b00)
16 Ub = sp.Matrix([[b00, b01], [b10, b11]])
17
18 c10 = - sp.exp(sp.I * phi_c) * sp.conjugate(c01)
19 c11 = sp.exp(sp.I * phi_c) * sp.conjugate(c00)
20 Uc = sp.Matrix([[c00, c01], [c10, c11]])
21
22
23 eye = sp.Matrix([[1, 0], [0, 1]]) # Identity
24
25 U1 = spq.TensorProduct(spq.TensorProduct(eye, eye), Uc)
26
27 U2 = sp.Matrix([[1, 0, 0, 0], [0, b00, 0, b01],
28                [0, 0, 1, 0], [0, b10, 0, b11]])
29 U2 = spq.TensorProduct(eye, U2)
30
31 U3 = sp.Matrix([[1, 0, 0, 0, 0, 0, 0, 0], [0, 0, 0, 0, 0, 1, 0, 0],
32                [0, 0, 1, 0, 0, 0, 0, 0], [0, 0, 0, 1, 0, 0, 0, 0],
33                [0, 0, 0, 0, 1, 0, 0, 0], [0, 1, 0, 0, 0, 0, 0, 0],
34                [0, 0, 0, 0, 0, 0, 1, 0],
35                [0, 0, 0, 0, 0, 0, 0, 1]])
36
37 U4 = spq.TensorProduct(spq.TensorProduct(Ua, eye), eye)
38
39 U5 = sp.Matrix([[1, 0, 0, 0, 0, 0, 0, 0], [0, 1, 0, 0, 0, 0, 0, 0],

```

```

40         [0, 0, 1, 0, 0, 0, 0, 0], [0, 0, 0, 1, 0, 0, 0, 0],
41         [0, 0, 0, 0, 0, 0, 1, 0], [0, 0, 0, 0, 0, 1, 0, 0],
42         [0, 0, 0, 0, 1, 0, 0, 0],
43         [0, 0, 0, 0, 0, 0, 0, 1]])
44
45     U6 = sp.Matrix([[b00, 0, b01, 0], [0, 1, 0, 0],
46                   [b10, 0, b11, 0], [0, 0, 0, 1]])
47     U6 = spq.TensorProduct(eye, U6)
48
49     # UcXUc
50     U7_00 = c01 * sp.conjugate(c00) + c00 * sp.conjugate(c01)
51     U7_01 = c01 * sp.conjugate(c10) + c00 * sp.conjugate(c11)
52     U7_10 = c11 * sp.conjugate(c00) + c10 * sp.conjugate(c01)
53     U7_11 = c11 * sp.conjugate(c10) + c10 * sp.conjugate(c11)
54
55     U7 = sp.Matrix([[1, 0, 0, 0, 0, 0, 0, 0], [0, 1, 0, 0, 0, 0, 0, 0],
56                   [0, 0, U7_00, U7_01, 0, 0, 0, 0],
57                   [0, 0, U7_10, U7_11, 0, 0, 0, 0],
58                   [0, 0, 0, 0, 1, 0, 0, 0], [0, 0, 0, 0, 0, 1, 0, 0],
59                   [0, 0, 0, 0, 0, 0, 1, 0],
60                   [0, 0, 0, 0, 0, 0, 0, 1]])
61
62     U = U7 * U6 * U5 * U4 * U3 * U2 * U1
63     sp.pprint(U)
64     sp.print_latex(U)

```



# Bibliography

- [1] Mateus Araújo, Fabio Costa, and Časlav Brukner. “Computational Advantage from Quantum-Controlled Ordering of Gates”. In: *Physical Review Letters* 113.25 (Dec. 2014). DOI: 10.1103/physrevlett.113.250402. URL: <https://doi.org/10.1103%2Fphysrevlett.113.250402>.
- [2] Mateus Araújo, Philippe Allard Guérin, and Ämin Baumeler. “Quantum computation with indefinite causal structures”. In: *Physical Review A* 96.5 (Nov. 2017). DOI: 10.1103/physreva.96.052315. URL: <https://doi.org/10.1103%2Fphysreva.96.052315>.
- [3] Mateus Araújo et al. “A purification postulate for quantum mechanics with indefinite causal order”. In: *Quantum* 1 (Apr. 2017), p. 10. ISSN: 2521-327X. DOI: 10.22331/q-2017-04-26-10. URL: <https://doi.org/10.22331/q-2017-04-26-10>.
- [4] Mateus Araújo et al. “Witnessing causal nonseparability”. In: *New Journal of Physics* 17.10 (Oct. 2015). DOI: 10.1088/1367-2630/17/10/102001. URL: <https://doi.org/10.1088%2F1367-2630%2F17%2F10%2F102001>.
- [5] Jonathan Barrett, Robin Lorenz, and Ognjan Oreshkov. “Cyclic quantum causal models”. In: *Nature Communications* 12.1 (Feb. 2021), p. 885. ISSN: 2041-1723. DOI: 10.1038/s41467-020-20456-x. URL: <https://doi.org/10.1038/s41467-020-20456-x>.
- [6] Jonathan Barrett, Robin Lorenz, and Ognjan Oreshkov. “Cyclic quantum causal models”. In: *Nature Communications* 12.1 (Feb. 2021). DOI: 10.1038/s41467-020-20456-x. URL: <https://doi.org/10.1038%2Fs41467-020-20456-x>.
- [7] Ämin Baumeler and Stefan Wolf. “The space of logically consistent classical processes without causal order”. In: *New Journal of Physics* 18.1 (Jan. 2016). DOI: 10.1088/1367-2630/18/1/013036. URL: <https://dx.doi.org/10.1088/1367-2630/18/1/013036>.
- [8] Charles H. Bennett et al. “Quantum nonlocality without entanglement”. In: *Physical Review A* 59.2 (Feb. 1999), pp. 1070–1091. DOI: 10.1103/physreva.59.1070. URL: <https://doi.org/10.1103%2Fphysreva.59.1070>.
- [9] Esteban Castro-Ruiz, Flaminia Giacomini, and Časlav Brukner. “Dynamics of Quantum Causal Structures”. In: *Phys. Rev. X* 8 (1 Mar. 2018). DOI: 10.1103/PhysRevX.8.011047. URL: <https://link.aps.org/doi/10.1103/PhysRevX.8.011047>.
- [10] Giulio Chiribella. “Perfect discrimination of no-signalling channels via quantum superposition of causal structures”. In: *Physical Review A* 86.4 (Oct. 2012). DOI: 10.1103/physreva.86.040301. URL: <https://doi.org/10.1103%2Fphysreva.86.040301>.



- [21] Lucien Hardy. "Probability Theories with Dynamic Causal Structure: A New Framework for Quantum Gravity". In: (Oct. 2005). DOI: 10.48550/ARXIV.GR-QC/0509120. URL: <https://arxiv.org/abs/gr-qc/0509120>.
- [22] Timothée Hoffreumon. "Processes with indefinite causal structure in quantum theory: The Multi-Round Process Matrix". MA thesis. ULB, 2019.
- [23] A. Jamiołkowski. "Linear transformations which preserve trace and positive semidefiniteness of operators". In: *Reports on Mathematical Physics* 3.4 (1972), pp. 275–278. ISSN: 0034-4877. DOI: [https://doi.org/10.1016/0034-4877\(72\)90011-0](https://doi.org/10.1016/0034-4877(72)90011-0). URL: <https://www.sciencedirect.com/science/article/pii/0034487772900110>.
- [24] Ravi Kunjwal and Āmin Baumeler. "Trading causal order for locality". In: (2022). arXiv: 2202.00440 [quant-ph].
- [25] M. S. Leifer and Robert W. Spekkens. "Towards a formulation of quantum theory as a causally neutral theory of Bayesian inference". In: *Physical Review A* 88.5 (Nov. 2013). DOI: 10.1103/physreva.88.052130. URL: <https://doi.org/10.1103/physreva.88.052130>.
- [26] Michael A. Nielsen and Isaac L. Chuang. *Quantum Computation and Quantum Information: 10th Anniversary Edition*. Cambridge University Press, 2010. DOI: 10.1017/CB09780511976667.
- [27] J. Niset and N. J. Cerf. "Multipartite nonlocality without entanglement in many dimensions". In: *Physical Review A* 74.5 (Nov. 2006). DOI: 10.1103/physreva.74.052103. URL: <https://doi.org/10.1103/physreva.74.052103>.
- [28] Ognjan Oreshkov. "Time-delocalized quantum subsystems and operations: on the existence of processes with indefinite causal structure in quantum mechanics". In: *Quantum* 3 (Dec. 2019), p. 206. ISSN: 2521-327X. DOI: 10.22331/q-2019-12-02-206. URL: <https://doi.org/10.22331/q-2019-12-02-206>.
- [29] Ognjan Oreshkov, Fabio Costa, and Časlav Brukner. "Quantum correlations with no causal order". In: *Nature Communications* 3.1 (Jan. 2012). DOI: 10.1038/ncomms2076. URL: <https://doi.org/10.1038/ncomms2076>.
- [30] Lorenzo M. Procopio et al. "Experimental superposition of orders of quantum gates". In: *Nature Communications* 6.1 (Aug. 2015). DOI: 10.1038/ncomms8913. URL: <https://doi.org/10.1038/ncomms8913>.
- [31] Giulia Rubino et al. "Experimental verification of an indefinite causal order". In: *Science Advances* 3.3 (Mar. 2017). DOI: 10.1126/sciadv.1602589. URL: <https://doi.org/10.1126/sciadv.1602589>.
- [32] William F. Stinespring. "Positive functions on \*-algebras". In: *Proc. Amer. Math. Soc.* 6, 211-216 (1955). DOI: <https://doi.org/10.1090/S0002-9939-1955-0069403-4>.
- [33] Julian Wechs. *Private communication*. 2022.
- [34] Julian Wechs, Cyril Branciard, and Ognjan Oreshkov. "Existence of processes violating causal inequalities on time-delocalised subsystems". In: *Nature Communications* 14 (Mar. 2023). DOI: 10.1038/s41467-023-36893-3.
- [35] Julian Wechs et al. "Quantum Circuits with Classical Versus Quantum Control of Causal Order". In: *PRX Quantum* 2 (3 Aug. 2021), p. 030335. DOI: 10.1103/PRXQuantum.2.030335. URL: <https://link.aps.org/doi/10.1103/PRXQuantum.2.030335>.

- 
- [36] Kejin Wei et al. "Experimental Quantum Switching for Exponentially Superior Quantum Communication Complexity". In: *Physical Review Letters* 122.12 (Mar. 2019). DOI: 10.1103/physrevlett.122.120504. URL: <https://doi.org/10.1103/physrevlett.122.120504>.
- [37] Wataru Yokojima et al. "Consequences of preserving reversibility in quantum superchannels". In: *Quantum* 5 (Apr. 2021), p. 441. ISSN: 2521-327X. DOI: 10.22331/q-2021-04-26-441. URL: <https://doi.org/10.22331/q-2021-04-26-441>.